AD-A128 365 SUBSONIC AND TURBULENT REACTIVE FLOWS(U) SCIENCE 1/1
APPLICATIONS INC MCLEAN VA K KAILASANATH ET AL. APR 83
SAI-84-128-WA SBI-AD-E001 442 N00014-82-C-2107
UNCLASSIFIED F/G 20/4 NL

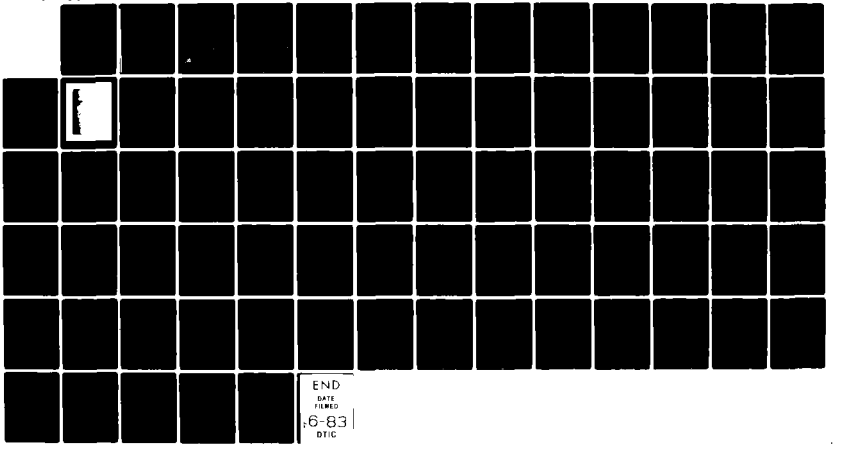

END
DATE FILMED
6-83
DTIC

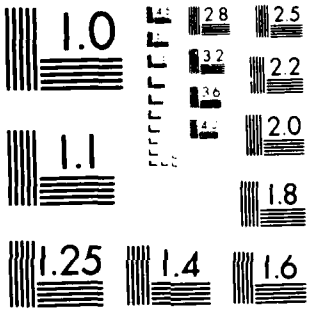

SUPERSONIC AND TURBULENT REACTIVE FLOWS

[illegible]

SAI-83-128-RA

(12)

SCIENCE APPLICATIONS, INC.

SUBSONIC AND TURBULENT REACTIVE FLOWS

FINAL REPORT

SAI 84-128-WA

(12)

SCIENCE APPLICATIONS, INC.

Post Office Box 1303, 1710 Goodridge Drive, McLean, Virginia 22102, (703) 821-4300

SUBSONIC AND TURBULENT REACTIVE FLOWS

FINAL REPORT

SAI 84-128-WA

Submitted To

Laboratory for Computational Physics
Naval Research Laboratory
Washington, D.C. 20375

Prepared Under

NRL Contract No. N00014-82-C-2107
SAI Project No. 1-157-18-555-00

Prepared by

Kazhikathra Kailasanath, Mark Fry, and Ellis Hyman

April 1983

SCIENCE APPLICATIONS, INCORPORATED
1710 Goodridge Drive, McLean, Virginia 22102

TABLE OF CONTENTS

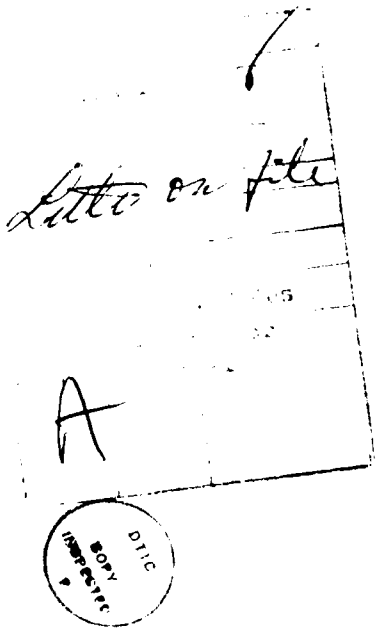

GENERAL DISCUSSION

The FAST2D code, a two-dimensional hydrocode developed by the Laboratory for Computational Physics at NRL, has been modified and used to model homogeneous flows. The speed of the transport algorithm which advances in time the density, momentum, and energy has been improved by a factor of two. This improved code has been used to model the transition to turbulence for shear flow.

When fluids of different densities flow at different relative velocities, one stream above another, an instability develops. The vorticity of a slab with a slight initial disturbance is positive for a positive velocity leading to a migration of positive vorticity. Where vorticity is displaced downwards a positive x component is induced. This accumulation will induce clockwise velocities which amplify the initial disturbance leading to the instability.

To model such a flow system a computational grid was chosen 200x64 in x and y, respectively. Zone sizes of 2.8cm in x and 1.0cm in y were used. Downstream the grid was stretched to obtain maximum length. To insure against spurious signals propagating upstream a special boundary condition was implemented. The momentum outflow was compared to the momentum inflow and adjusted to obtain a balanced flow. This boundary condition was checked for several flow velocities to insure a consistent answer.

The outflow boundary value for the pressure was chosen in the following manner. To insure that the average pressure does not greatly deviate from the ambient pressure, the outflow pressure must act so as to restore the computed pressure to ambient. Therefore, we assert that the condition

$$P_{outflow} = P_{ambient}$$

would be an overly harsh restoring condition, if, for example $P \geq 1.05\ P_{ambient}$ or $P < 0.95\ P_{ambient}$. The gradient $P\text{-}P_{ambient}/\Delta Y$ has associated with it some characteristic scale length. If ℓ is the width of our system such a length might be $\ell/2$, then

$$P_{outflow} = \frac{2\Delta Y}{\ell} (P_{ambient}\text{-}P) + P$$

Take the case where $P > P_{ambient}$, then $P_{outflow} < P$ which creates a positive gradient allowing flow out. The case where $P < P_{ambient}$ allows $P_{outflow} > P$ causing a negative gradient so as to increase P.

An important part of studying the development of the instability is analyzing the data. The graphics routines were modified and enhanced to establish a color presentation capability. A shadow plotter was used as the basis for the density plotter. A vector velocity plotter was modified to present arrows in color. Figure 1 shows the resulting display of density and velocity for the problem at 1.72 milliseconds.

Several preliminary calculations were completed to test the overall production ability of the code with the new boundary conditions and the new data presentation. Study of these co-flowing problems requires many sets of configurations, and thus the ability to produce a complete simulation every five to six days including color processing time. This requirement has been met and the code is now ready for that use.

For the subsonic reactive flow part of the program, the following three tasks were performed:

(1) the one-dimensional time-dependent flame model was adapted to include a capability for modeling the thermal diffusion phenomena,

(2) a study of the effects of thermal diffusion on the burning velocity of hydrogen-air mixtures was carried out, and

(3) the flame code has been documented as NRL Memorandum Report 4910.

Subsonic Reactive Flows

In the past[1], SAI in collaboration with NRL had modified and used the NRL Flame code[2] to study the ignition and quenching of pre-mixed gases[3] and for the determination of the burning velocity of fuel-air mixtures[4]. It was also suggested[4] earlier that the thermal diffusion phenomena might play a significant role in the burning of hydrogen-air mixtures. During this contract year, the flame code has been extended to include the thermal diffusion phenomena and the effect of thermal diffusion on the burning velocity of a stoichiometric hydrogen-air mixture has also been studied. A detailed account of this work is included in this report in Appendix A and a brief description is given below.

Thermal diffusion contributes an additional source term [see Eq. (8) in App. A] to the diffusion equations [Eq. (7) in App. A] and in this way changes the diffusion velocity of the various species in the system. It also modifies the energy equation [Eq. (4) in App. A] by contributing a term to the heat flux vector [Eq. (5) in App.A]. The evaluation of these terms and the solution of the diffusion and energy equations is discussed in detail in Appendix A. In the discussion below, the source terms in the diffusion equations due to thermal diffusion will be represented as S_{TD} and those due to ordinary diffusion (due to concentration gradients) as S_{OD}.

In order to evaluate the importance of thermal diffusion, the burning velocity of a hydrogen-air mixture was determined with and without considering the source terms due to thermal diffusion. The net effect of thermal diffusion is to lower the burning velocity of a stoichiometric hydrogen-air mixture by about 7%. In order to understand the reasons for this effect, the spatial variation of the terms S_{OD} and S_{TD} for the various species have been calculated for a steady propagating flame. For the species O_2, the term S_{TD} is opposite in sign to S_{OD}. A negative value for S_{TD} implies that the oxygen molecules are diffusing from the hotter region to the cooler region. Since the sum of the two source terms determines the diffusion velocity, the effect of thermal diffusion is to slow the diffusion of O_2 molecules into the higher temperature region of the flame. The effect of this on the burning velocity is not obvious since it depends on the details of the reaction mechanism and the distribution of other species. For the species N_2, the term S_{TD} is comparable to the term S_{OD} and the effect of thermal diffusion is to enhance the movement of N_2 from the hotter region of the flame to the cooler region. For the species H_2, the effect of thermal diffusion is similar to that of ordinary diffusion and it enhances the movement of H_2 from the cooler region to the hotter region.

The term S_{OD} for the species H is particularly interesting. It is observed that the H atoms in a certain region of the flame (the region with T > 1400 K for the flame studied here) have a tendency to diffuse into the hotter region while the rest (in the region with T < 1400 K) diffuse into the cooler region. The diffusion of H atoms into the cooler region is very important in the propagation of the flame. The effect of thermal diffusion is to delay and decrease the diffusion of H atoms into the cooler region. Since the H atoms are produced primarily in the high temperature region, the thermal diffusion of H atoms can significantly retard the rate of propagation of the flame. This may be the main reason for the observed reduction in the burning velocity when the effects of thermal diffusion were included. This has been discussed in more detail in Section 5.2 of Appendix A.

The model used for the flame studies discussed above and elsewhere[1-4] is a one-dimensional, time-dependent, Lagrangian numerical model. The model incorporates a number of new approaches and algorithms which have been tested by comparisons to less complex or analytic solutions and by comparisons to experimental data. These new approaches and algorithms along with the input parameters required by the model have been discussed in the NRL Memorandum Report 4910

entitled "A One-Dimensional Time-Dependent Model for Flame Initiation, Propagation and Quenching." This memorandum report has been included in this report as Appendix A.

REFERENCES

1. "Fluid Dynamics-Reactive Flow Modeling" Final Report No. SAI-82-655-WA.
2. Oran, E.S. and Boris, J.P., "Theoretical and Computational Approach to Modeling Flame Ignition," NRL Memorandum Report 4131 (1979). Also appears in Progress in Astronautics and Aeronautics, Vol. 76, pp 154-171 (1981).
3. Kailasanath, K., Oran, E.S. and Boris, J.P., "A Theoretical Study of the Ignition of Premixed Gases," Combust. Flame 47:173-190 (1982).
4. Kailasanath, K., Oran, E.S., Boris, J.P. and Young, T.R., "Time-Dependent Simulation of Flames in Hydrogen-Oxygen-Nitrogen Mixtures," in Numerical Methods in Laminar Flame Propagation (Eds: N. Peters and J. Warnatz) pp. 152-166.

FIGURE CAPTIONS

Fig. 1. Material densities and vector velocities.

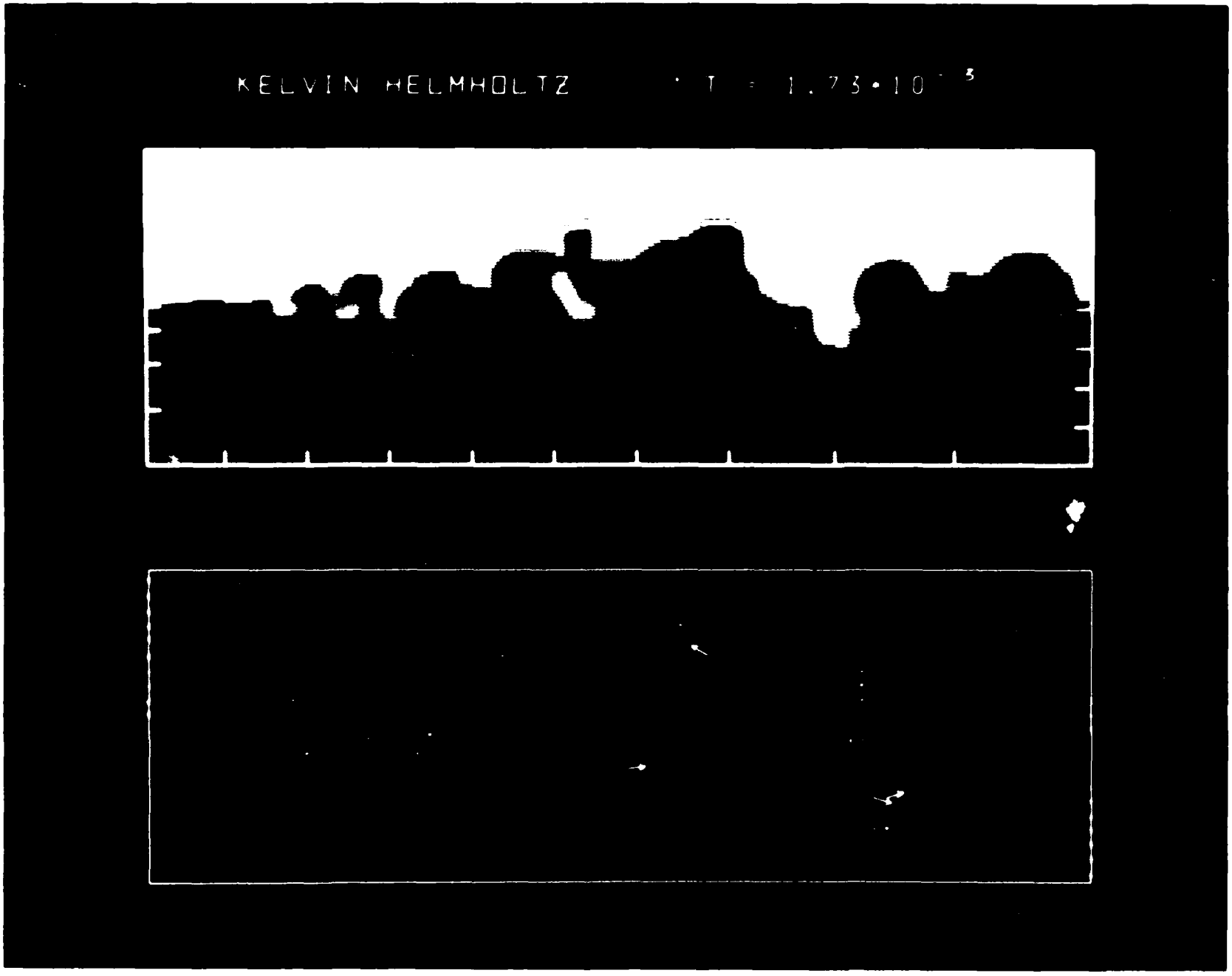
KELVIN HELMHOLTZ
T = 1.73•10 3

APPENDIX A

A ONE-DIMENSIONAL TIME-DEPENDENT MODEL FOR FLAME INITIATION, PROPAGATION AND QUENCHING

NRL Memorandum Report 4910

A One-Dimensional Time-Dependent Model for Flame Initiation, Propagation and Quenching

K. KAILASANATH*, E. S. ORAN, AND J. P. BORIS

Laboratory for Computational Physics

**Science Applications, Inc.,*
McLean, VA 22102

September 30, 1982

This work was sponsored by the Office of Naval Research and the Naval Material Command.

NAVAL RESEARCH LABORATORY
Washington, D.C.

SECURITY CLASSIFICATION OF THIS PAGE (When Data Entered)

REPORT DOCUMENTATION PAGE	READ INSTRUCTIONS BEFORE COMPLETING FORM
1 REPORT NUMBER: NRL Memorandum Report 4910	2 GOVT ACCESSION NO. / 3 RECIPIENT'S CATALOG NUMBER
4 TITLE (and Subtitle): A ONE-DIMENSIONAL TIME-DEPENDENT MODEL FOR FLAME INITIATION, PROPAGATION AND QUENCHING	5 TYPE OF REPORT & PERIOD COVERED: Interim report on a continuing project. / 6 PERFORMING ORG. REPORT NUMBER
7 AUTHOR(s): K. Kailasanath*, E.S. Oran and J.P. Boris	8 CONTRACT OR GRANT NUMBER(s)
9 PERFORMING ORGANIZATION NAME AND ADDRESS: Naval Research Laboratory, Washington, DC 20375	10 PROGRAM ELEMENT, PROJECT, TASK AREA & WORK UNIT NUMBERS: 62543; SF-43-400-391; 44-0061-A-2
11 CONTROLLING OFFICE NAME AND ADDRESS: NAVMATSYSCOM/NSRDC	12 REPORT DATE: September 30, 1982 / 13 NUMBER OF PAGES: 57
14 MONITORING AGENCY NAME & ADDRESS(if different from Controlling Office)	15 SECURITY CLASS. (of this report): UNCLASSIFIED / 15a DECLASSIFICATION DOWNGRADING SCHEDULE

16 DISTRIBUTION STATEMENT (of this Report)

Approved for public release; distribution unlimited.

17 DISTRIBUTION STATEMENT (of the abstract entered in Block 20, if different from Report)

18 SUPPLEMENTARY NOTES

*Present address: Science Applications, Inc., McLean, VA 22102.

This work was sponsored by the Office of Naval Research and the Naval Material Command.

19 KEY WORDS (Continue on reverse side if necessary and identify by block number)

Numerical simulations
Flames
Combustion
Hydrogen combustion

20 ABSTRACT (Continue on reverse side if necessary and identify by block number)

This report describes a one-dimensional, time-dependent, Lagrangian numerical model developed to study the initiation, propagation and quenching of laminar flames. A number of new approaches and algorithms as well as input parameters used in the model are discussed. Calculations of initiation and minimum ignition energies in hydrogen-oxygen-nitrogen mixtures are presented along with calculations of the burning velocity of hydrogen in air.

DD FORM 1 JAN 73 1473 EDITION OF 1 NOV 65 IS OBSOLETE
S/N 0102-014-6601

SECURITY CLASSIFICATION OF THIS PAGE (When Data Entered)

CONTENTS

A ONE-DIMENSIONAL TIME-DEPENDENT MODEL FOR FLAME INITIATION, PROPAGATION AND QUENCHING

1. INTRODUCTION

This report describes a one-dimensional, time-dependent, Lagrangian numerical model developed to study the initiation, propagation and quenching of laminar flames. The model incorporates a number of new approaches and algorithms which have now been tested by comparisons to less complex or analytic solutions and by comparisons to experimental data. These new elements include: ADINC [1] an implicit, Lagrangian method for solving the convective parts of the conservation equations; DFLUX [2,3] a variable accuracy algorithm for determining diffusion fluxes without having to invert matrices; VSAIM, a vectorized version of the ordinary differential equation solver, CHEMEQ [4,5]; and a new method for treating an open boundary in an implicit, Lagrangian calculation. An asymptotic coupling method is used in conjunction with timestep splitting to couple the various physical and chemical processes. This approach allows the use of entirely different algorithms for the physical processes represented by the different terms in the conservation equations.

Manuscript submitted July 26, 1982.

The model has been used for a variety of flame studies of hydrogen-oxygen-nitrogen mixtures. These include calculations of minimum ignition energies [6,7], flammability limits [8], quench volumes [7], and burning velocities [9]. The chemical rate scheme has now been tested extensively, as have the input parameters for the transport properties. Thus we expect the model to calculate correctly the time-dependent behavior implied by the initial and boundary conditions supplied.

After a brief review of related literature, a summary is given of the important numerical features of the model. Then several calculations are presented. The first is a flame initiation and minimum ignition energy study of a mixture of $H_2:O_2:N_2/2:1:10$ initially at 298 K and 1 atm. This is inherently a time-dependent problem and takes advantage of this property of the model. The second problem discussed is a calculation of the burning velocity of the mixture $H_2:O_2:N_2/2:1:4$, again at 298 K and 1 atm. The burning velocity describes a steady state property of the system; thus we show below that the model also does well on this type of calculation.

2. BACKGROUND

The laminar flame problem is the earliest combustion problem to be studied theoretically which required the simultaneous consideration of both fluid dynamics and chemical kinetics for its solution [10]. The problem of determining the propagation velocity of a deflagration wave was first studied by Mallard and LeChatelier [11]. Since then there have been many analytical attempts, [e.g. 12, 13] with varying degrees of complexity and approximation, to study simple steady flames. Some of these have been summarized by Williams [10]. Whereas these analytical techniques are extremely informative, they cannot satisfactorily describe the detailed structure of flames since they all include very approximate chemical kinetic schemes and transport properties. For this one has to resort to numerical methods.

One of the first attempts to solve the laminar flame problem numerically was that of Hirschfelder and co-workers [14]. They formulated the unsteady flame problem as a system of three-dimensional nonlinear partial differential equations and they solved the one-dimensional steady flame as a two point boundary value problem. They used approximate methods to estimate the mass flow rate which is the eigenvalue of the two-point boundary value problem and then used a numerical shooting method to obtain the temperature and species profiles. Although the first problem they studied involved only single step kinetics, they later applied the same solution procedure to study flames for which the kinetics involved chain reactions [15,16].

In 1956, Spalding [17] applied a time-dependent system of nonlinear partial differential equations using explicit finite-difference techniques to

study hydrazine flames. He assumed initial profiles for the temperature and species concentrations and obtained the steady state burning velocity by carrying out the computations for a sufficiently long time. Spalding's method was subsequently used by Adams and Cook [18] to study the effect of pressure on the reaction mechanism and speed of hydrazine flames, and by Dixon-Lewis [19] to study rich hydrogen-oxygen flames. Dixon-Lewis [19] used a set of fourteen reactions to describe hydrogen-oxygen kinetics, but assumed a steady state approximation for the radical distribution in the flame. In 1968, Dixon-Lewis [20] studied the flame structure and flame reaction kinetics of hydrogen-oxygen-nitrogen flames using detailed expressions for the diffusive transport coefficients in multicomponent systems. He also used this time-dependent numerical model to study ignition by localized sources [21].

The work of Dixon-Lewis and co-workers described above proved the one-dimensional unsteady flame with complex chemistry and detailed diffusive transport coefficients could be solved using numerical methods. The emphasis then shifted toward the development of more economical and improved numerical methods. In 1971, Spalding, et al. [22] presented an implicit-finite difference method in which the unsteady flame equations were transformed to a form which could be solved by a numerical method developed by Patankar and Spalding [23] for two dimensional boundary layer equations. They used simplified transport properties [14] and a four step chain reaction mechanism to study the propagation of hydrogen-bromine flames [24]. However this method requires careful ordering of the solution of the equations, and a certain manner of linearizing the source terms. The same numerical procedure was used later by Tsatsaronis [25] to study unsteady flame propagation in

methane, oxygen, nitrogen mixtures using very detailed chemical kinetic mechanisms and transport properties.

The kinetics and propagation of methane-air flames was studied by Smoot et al. [26] using a mixed explicit-implicit finite difference technique. The diffusive transport terms were solved explicitly and the kinetic terms were solved using linearized implicit techniques. Bledgian [27] employed a method of lines technique where the nonlinear parabolic initial-boundary value problem is reduced to a set of nonlinear first order initial value problems. Sophisticated initial value problem integrators were used to solve the resulting ordinary differential equations system. Instead of using finite difference approximations to discretize the spatial derivative, Margolis [28] used a spline collocation procedure in his method of lines approach. Westbrook and Dryer [29] have deduced a comprehensive reaction mechanism for methanol oxidation involving eighty four reactions using an implicit finite-difference algorithm [30] to solve the unsteady flame equations. They used simplified expressions for the diffusive transport coefficients which were adjusted to give good laminar flame speed prediction for methane-air flames

Dixon-Lewis has more recently used a composite flux method [31] to study a variety of problems like the kinetic mechanism, structure and propagation of flames in hydrogen-oxygen-nitrogen flames [32] and flame inhibition by organic halogen compounds [33]. He discusses the ranges of applicability of the partial equilibrium and quasi-steady assumptions in relation to the distribution of radical populations in the flames [32].

Warnatz has extensively studied both freely propagating and burner stabilized flames in a variety of premixed gases [34, 35, 36, 37, 38]. He

linearizes the chemical reaction terms and solves the time-dependent equations implicitly with assumed initial guesses for the temperature and species profiles. He also uses a simplified transport model [34] which agrees well with the complete multicomponent formulation of diffusion and thermal conduction. In his recent study [38] of the concentration, pressure and temperature dependence of the flame velocity in hydrogen-oxygen-nitrogen mixtures he concludes that at the present state of knowledge predictions of laminar, premixed flame propagation should be as reliable as experimental results.

Coffee and Heimerl, using a method of lines approach [39] examined different methods of approximating multispecies transport phenomena in models of premixed, laminar, steady-state flames. They concluded that the selection of the input values for the individual species transport properties is more important than the selection of the approximation method [40].

There have also been a number of approaches which solve a steady state formulation of the flame equations. These include the works of Dixon-Lewis [41], Wilde [42] and Smooke [43]. The advantages and the difficulties in using steady state solution procedures have been discussed by Smooke [43]. These methods are good for obtaining burning velocities and steady state profiles, but cannot provide information on the ignition and development of flames.

The model presented in this report solves the time-dependent partial differential equations and hence can describe the initiation, propagation and quenching of laminar flames. It uses detailed chemical kinetic models without any steady state or quasi-equilibrium assumptions and so can be used to study all laminar premixed flames. It uses an asymptotic coupling method in conjunction with timestep splitting to couple the various physical and

chemical processes. This approach allows the use of entirely different algorithms for the processes represented by the different terms in the conservation equations. Thus it is numerically very efficient and inexpensive. A Lagrangian formulation is used in order to maintain steep gradients for a long period of time. The model has been used for a variety of flame studies of hydrogen-oxygen-nitrogen mixtures. These include calculations of minimum ignition energy [6,7], flammability limits [8], quench volumes [7], and burning velocities [9].

3. NUMERICAL MODEL

3.1 Basic Equations

We solve the time-dependent equations for conservation of total mass density ρ, momentum $\rho\underline{v}$, and energy density E_m as well as the individual species number densities $\{n_j\}$. These may be written as [2,10]:

$$\frac{\partial \rho}{\partial t} = -\underline{\nabla}\cdot\rho\underline{v} \tag{1}$$

$$\frac{\partial n_j}{\partial t} = -\underline{\nabla}\cdot n_j\underline{V}_j - \underline{\nabla}\cdot n_j\underline{v} + P_j - L_j n_j \tag{2}$$

$$\frac{\partial \rho\underline{v}}{\partial t} = -\underline{\nabla}\cdot(\rho\underline{v}\underline{v}) - \underline{\nabla} P + \underline{\nabla}\cdot\eta_m\left[\underline{\nabla}\underline{v} + (\underline{\nabla}\underline{v})^T\right] \tag{3}$$

$$\frac{\partial E_m}{\partial t} = -\underline{\nabla}\cdot E\underline{v} - \underline{\nabla}\cdot P\underline{v} - \underline{\nabla}\cdot\underline{Q} \tag{4}$$

where the heat flux vector, $\underline{Q}$, is defined as

$$\underline{Q} = -\lambda_m\underline{\nabla} T + \sum_j n_j h_j \underline{V}_j + P\sum_j K_j^T \underline{V}_j \tag{5}$$

The quantity $\underline{v}$ is the fluid velocity, the $\{\underline{V}_j\}$ are the diffusion velocities, and $\{P_j\}$ and $\{L_j\}$ refer to the chemical production and loss processes for the individual species j. The quantities η_m and λ_m are the mixture viscosities and thermal conductivities respectively. The superscript "T" in the last term of Eq. (3) indicates that the transpose is taken. The quantity E in Eq. (4) is the total energy E_m minus the total heat of formation. The quantities $\{h_j\}$ are the temperature dependent enthalpies for

each species, and the $\{D_{jk}\}$ and $\{K_j^T\}$ are the sets of binary diffusion coefficients and thermal diffusion ratios, respectively.

We also assume that the mixture behaves like an ideal gas so that the pressure, P, may be written as:

$$P = NkT \tag{6}$$

where N is the total number density, k_B is Boltzmann's constant and T is the temperature. The model presented in this report, however, is not restricted to ideal gases and in fact any equation of state may be used.

The diffusion equations may be written as

$$S_j = \sum_k \frac{n_j n_k}{N^2 D_{jk}} (\underline{V}_k - \underline{V}_j) \tag{7}$$

where the source terms S_j are defined as

$$S_j = \underline{\nabla}\left(\frac{n_j}{N}\right) - \left(\frac{\rho_j}{\rho} - \frac{n_j}{N}\right) \frac{\underline{\nabla}P}{P} + K_j^T \frac{\underline{\nabla}T}{T} \tag{8}$$

The diffusion velocities are also subject to the constraint:

$$\sum_j \rho_j \underline{V}_j = 0 \tag{9}$$

Below we describe the basic features of the solution techniques adopted to solve the terms representing the chemical reactions, the convective and diffusive transport processes, and techniques for coupling the solutions of the equations representing these processes.

3.2 Convective Transport

The convective transport terms in Eqs. (1-4) are solved by the algorithm ADINC [1]. ADINC, designed for either Adiabatic or incompressible flows, is an implicit, Lagrangian algorithm. Since ADINC communicates compression and expansion across the system implicitly, it overcomes the Courant time-step limit. Since it is Lagrangian, it can maintain steep gradients computationally for a long period of time. This is important in flame calculations where the diffusive transport of material and energy can govern the system evolution and therefore must be calculated accurately.

ADINC solves the following equations for mass and momentum transport in one dimension:

$$\frac{d\rho}{dt} = - \rho \, \nabla \cdot \underline{v} \qquad (10)$$

$$\rho \frac{d\underline{v}}{dt} = - \nabla P \qquad (11)$$

The energy evolution equation is eliminated by using an adiabatic equation of state:

$$\rho(P,S) = \rho_c + (P/S)^{1/\gamma} \qquad (12)$$

This equation of state with $\rho_c = 0$ is correct for adiabatic compression and expansion of an ideal gas. The entropy, S, is assumed constant throughout the numerical integration. Non-adiabatic processes, such as external heating, thermal conduction and chemical energy release, are added to Eqs. (10-11) using the timestep splitting methods described below.

Given an aproximation to the pressure, ADINC calculates the fluid density using Eq. (12). This equation-of-state density is compared to the density derived from the fluid dynamics through Eq. (10). The difference is

iterated to zero using a quadratically convergent implicit solution of Eq. (11) which then gives an improved approximation to the pressure. During this iteration the analytic derivative dA/dP is used where A is the volume of a computational cell. Thus

$$\frac{1}{A}\frac{dA}{dP} = -\frac{1}{\gamma\rho P}(P/S)^{1/\gamma} \qquad (13)$$

for the particular equation of state (12).

ADINC assumes that pressure and density are constant within each individual finite-difference cell and that the physics is evolving slowly enough for full communication across that cell to have occurred in a timestep. When the densities in adjacent cells are different, the pressure gradient between the two cells will impart a different acceleration to the fluid just to the right and to the left of the interface between the two cells. If the fluid were permitted to move according to these distinct accelerations, the fluid would either overlap or a gap would appear at the interface after a short while. To prevent this, ADINC matches the acceleration calculated from the left to that from the right. This is described in more detail by Boris [1].

Problems can be set up in one of four geometries: cartesian coordinates, cylindrical coordinates, cylindrical coordinates, spherical coordinates and a variable power series coordinates for treating one-dimensional nozzle like geometries. The boundary conditions are controlled by specifying the position and velocity of the first and last cell interface.

3.3 Chemical Kinetics Calculations

The coupled, nonlinear, ordinary differential equations which describe the chemical interactions are taken from that part of Eq. (2) which represents the production and loss of reacting species:

$$\frac{\partial n_j}{\partial t} = P_j - L_j n_j \quad , j = 1, \ldots, M, \qquad (14)$$

where M is the total number of species present. The functional dependencies of the terms

$$P_j = P_j\{n_k(t)\}$$

$$L_j = L_j\{n_k(t)\} \quad , k = 1, \ldots, M \qquad (15)$$

emphasize the strong coupling between the various species. The system represented by Eq. (14) may be stiff when there are large differences in the time constants associated with different chemical reactions. Stiffness may occur for different species, in different locations, at different times or simultaneously throughout the course of an integration. Because of this, when there are a large number of reactions, the solution of the chemical kinetics equations is usually the most expensive part of a detailed reactive flow calculation. Furthermore, the computational cost increases with the number of species and the dimensionality of the problem. Therefore a method which is efficient, accurate, conservative, stable and which does not require storage of large quantities of data from one timestep to another is required. Such a method is VSAIM, which is a fully vectorized version of the selected asymptotic integration method employed in CHEMEQ [4,5].

In VSALM, the stiff equations are identified and solved using a very stable asymptotic method while the remaining equations are solved using a standard classical method. Since it is self starting and does not require matrix inversion, it is inexpensive. Species densities at only one time level are needed. Accuracy may be controlled by predetermined convergence parameters which control the stiffness criterion, the timestep, and thus effectively the degree of conservation. The method is stable for large timesteps and is vectorized for use in parallel processing computers.

3.4 Diffusive Transport

The diffusive transport processes considered in this model are molecular diffusion, thermal diffusion and thermal conduction. These are the parts of Eqs. (2,4) which are represented by the expressions:

$$\frac{\partial n_i}{\partial t} = - \underline{\nabla} \cdot n_i \underline{V}_i \tag{16}$$

$$\frac{\partial E}{\partial t} = - \underline{\nabla} \cdot \left[-\lambda \underline{\nabla} T + \sum_j h_j n_j \underline{V}_j + P \sum_j K_j^m \underline{V}_j \right] \tag{17}$$

These processes are crucial to the description of flame ignition and propagation since they are the mechanism by which heat and reactive species are transported ahead to the unburned gas. The effects of viscosity have not been considered in this paper.

The diffusion velocities $\{V_i\}$ in Eqs. (16, 17) are determined by solving the equations [2,44]

$$S_j = \sum_{\substack{k=1 \\ k \neq j}}^{M} \frac{n_j n_k}{N^2 D_{jk}} (\underline{V}_k - \underline{V}_j) = \underline{\nabla} (n_j/N) + K_j^m \frac{\nabla T}{T} \tag{18}$$

subject to the constraints

$$\sum_{j=1}^{M} S_j = 0, \text{ and } \sum_{j=1}^{M} \rho_j V_j = 0. \qquad (19)$$

An iterative algorithm, DFLUX, enables us to obtain the diffusion velocities without the cost of performing matrix inversions [2,3]. This method is of $O(M^2)$ and is vectorized. Thus it is substantially faster than $O(M^3)$ matrix inversions when four or more species are involved.

The Eqs. (16,17) are conservatively differenced and solved explicitly. Solving these equations requires knowledge of the binary diffusion coefficients D_{jk}, the thermal diffusion ratios K_j^T and the thermal conductivity λ. Representations of these coefficients which are easily used in reactive flow models and do not require the expensive inversion of matrices are chosen and these are discussed in a subsequent section of this report.

2.5 Timestep Splitting

In the asymptotic timestep split approach [2], the individual terms in the Eqs. (1-4) are solved independently as described above and then asymptotically coupled together. Since both chemistry and sound waves are usually stiff in deflagration problems, special care is required in coupling the chemical heat release to the fluid dynamics. In a flame, fluid dynamic expansion and diffusive transport relieve the pressure from the flame region as fast as it is generated. Thus the pressure stays effectively constant. Small pressure fluctuations, $O(v^2/c^2)$, do exist and are just large enough to drive the flows which reapportion the energy released by chemistry or transported by diffusive processes.

The energy released in chemcal reactions and that transported by diffusion and thermal conduction are converted to effective pressure changes as described below. Before the fluid dynamic timestep, the sum of all these pressure changes is added to the old pressure distribution to obtain a new pressure distribution. This new pressure distribution is used to modify the cell entropies. The new pressure distribution and cell entropies are used in the convection transport algorithm, ADINC to obtain the convect fluid expansion as described earlier.

The chemistry step should be taken at constant pressure, but if the profiles change slowly per timestep, it may also be taken at constant volume with temperature held fixed. On completion of the chemistry integration, the heat release is converted to an effective pressure change at constant volume because the cell volume has been held fixed during the chemical kinetics calculation. The chemical energy released can be calculated from the heats of formation and the changes in the number densities of the various species. Defining an energy density ε by:

$$\varepsilon = E_T - \frac{1}{2}\rho V^2 - \sum_j h_{o_j} n_j \qquad (20)$$

at the end of each chemical time step we have

$$\varepsilon(t+\Delta t) = \varepsilon(t) + \sum_j (n_j(t+\Delta t) - n_j(t)) h_{o_j} \qquad (21)$$

The changes in the number densities are calculated by solving the chemical rate equations as described in an earlier section of this report. Using the definition of enthalpy, the energy density ε is written as:

$$\varepsilon = \sum_j h_j(T) n_j - P. \qquad (22)$$

The temperature at the end of the chemical time step is evaluated from

Eq. (22) using the new values for ε and n_j and the temperature dependence of the sensible enthalpy h_j. Since Eq. (22) is highly nonlinear in temperature, a Newton-Raphson iteration technique is used and it usually converges in one or two iterations. This is the temperature that would have been attained if the entire energy released goes into heating the fluid. Since the chemical energy released also goes into fluid expansion, it would be incorrect to use this as the temperature for the next timestep. Therefore, the energy released is converted to an effective pressure change as

$$\Delta P = k_B T \sum_j n_j - P_{old} \qquad (23)$$

where T is the temperature calculated from Eq. (22) and n_j are the new number densities of the various species. The energy transported by thermal conduction and diffusion are also converted to effective pressure changes by using the equation

$$\Delta P = \Delta E \, (\gamma - 1) \qquad (24)$$

These pressure changes are used as energy source terms for the fluid dynamic timestep as described above.

3.6 Open Boundary Condition

In the study of unconfined flames, a representation for the open-boundary is required since the size of the computational domain is limited. One approach is to allow the computational cells to increase in size as they get further from the flame. Thus the computational domain is very large and there is no corresponding increase in computer storage. However, the cell stretching should be gradual to limit inaccuracies which arise as a result of

the varying cell size. Furthermore, adaptive gridding will be essential with this approach, since as the flame front moves toward the large cells, the resolution will have to decrease around the flame.

A second approach which we have used to study the propagation of unconfined flames takes advantage of the observation that the effect of an open boundary is to keep the pressure essentially constant. Therefore, in this approach the movement of the cell boundary that is on the open end is calculated by allowing the pressure in each cell at the end of a timestep to relax adiabatically to the pressure before the timestep. In practice this is done by calculating the changes in the cell volume V_c, by

$$V_c(t+\Delta t) = V_c(t)\left[\frac{P_{new}}{P(t)}\right]^{1/\gamma} \tag{25}$$

where

$$P_{new} = P(t) + \Delta P \tag{26}$$

and (ΔP) is the change in the presure due to diffusive transport, energy released in chemical reactions and any energy addition to the system. The changes in the volume of the cells causes the location of the open boundary to change. The location of the open boundary and the fluid velocity in the last cell (which is also the velocity of the open boundary) are used as open boundary conditions to the convective transport algorithm ADINC.

4. EVALUATION OF MATERIAL PROPERTIES

In order to apply the numerical model described above, we need expressions for the diffusive transport coefficients, the enthalpies of the various species involved, the chemical kinetic rate scheme and the reaction rate constants. In this section we first present general equations for the evaluation of some of these material properties and then present the input parameters used for the study of pre-mixed hydrogen-oxygen-nitrogen systems.

4.1 General Expressions

The diffusive transport coefficients presented here have been taken with some modification from the summary by Picone [45]. The forms given are for mixtures of neutral gases. Their derivations are based on or are extensions of the fundamental work of Chapman and Cowling [44] and Hirschfelder, Curtis and Bird [46].

4.1.1 Thermal Conductivity

For the mixture thermal conductivity, an extremely useful equation has been given by Mason and Saxena [47]:

$$\lambda_m = \sum_j \lambda_j \left[1 + \frac{1.065}{2\sqrt{2}\, n_j} \sum_{k \neq j} n_k \Phi_{jk}\right]^{-1} \qquad (21)$$

where λ_j is the thermal conductivity of a pure polyatomic gas of species j, and Φ_{jk} is given by

$$\Phi_{jk} = \frac{\left[1 + \left(\frac{\lambda_j^0}{\lambda_k^0}\right)^{1/2} \left(\frac{M_k}{M_j}\right)^{1/4}\right]^2}{\left[1 + \frac{M_j}{M_k}\right]^{1/2}} \qquad (22)$$

where λ_j^0 is the thermal conductivity of gas j if it is monatomic, or it is the thermal conductivity of a polyatomic gas with internal degrees of freedom "frozen", and M_j is the atomic mass of species j. The thermal conductivity, λ_j of a pure polyatomic gas can be estimated from the monatomic thermal conductivities λ_j^0 by using the modified Eucken factor [48], F_j, as

$$\lambda_j = F_j \lambda_j^0 \tag{29}$$

where

$$F_j = 0.115 + 0.354 \frac{C_{p_j}}{k_B} \tag{30}$$

and C_{p_j} is the molecular specific heat at constant pressure. The $\{\lambda^0_j\}$ may be written as

$$\lambda_j^0 = \frac{8.322 \times 10^3}{\sigma_j^2 \Omega_{jj}^{(2,2)*}} \left(\frac{T}{M_j}\right)^{1/2} \tag{31}$$

where $\Omega_{jj}^{(2,2)*}$, a collision integral normalized to its rigid sphere value is a function of T_j^*, is the reduced temperature given by

$$T_j^* = \frac{k_B T}{\varepsilon_j} . \tag{32}$$

The terms σ_j and ε_j are force constants in the potential function which describes the interaction between two molecules of the same species, j.

4.1.2 Ordinary Diffusion Coefficients

We assume that the "ordinary" (concentration) diffusion coefficients for a pair of species (j,k) in a multicomponent mixture is to a first approximation equal to that in a binary mixture of species j and k. For some binary mixtures of dilute gases, Mason and Marrero [49] have given a semi-empirical

expression which describes the variation of D_{jk} over a wide temperature range. Their expression for D_{jk} can be written as

$$D_{jk} = \frac{A_{jk} T^{B_{jk}}}{N} . \tag{33}$$

When the coefficients A_{jk} and B_{jk} are not available, the D_{jk} may be estimated from

$$D_{jk} = \frac{2.628 \times 10^{-3}}{P \sigma_{jk}^2 \Omega_{jk}^{(1,1)*}} \left[\frac{T^3 (M_j + M_k)}{2 M_j M_k} \right]^{1/2} \tag{34}$$

where $\Omega_{jk}^{(1,1)*}$, a collision integral normalized to its rigid sphere value is a function of the reduced temperature

$$T^*_{jk} = \frac{k_B T}{\varepsilon_{jk}} \tag{35}$$

The factors σ_{jk} and ε_{jk} in the above equation are force constants in the potential function which describes the interactions between molecules of species j and k. In most cases values of σ_{jk} and ε_{jk} are not available and are usually calculated from

$$\sigma_{jk} = \frac{1}{2} (\sigma_j + \sigma_k) \tag{36}$$

and

$$\varepsilon_{jk} = (\varepsilon_j \varepsilon_k)^{1/2}. \tag{37}$$

4.1.3 Thermal Diffusion Ratios

Thermal diffusion is a second order effect [44, 46] which is only of importance when there are large differences between the atomic masses of constituent species. An expression for the thermal diffusion ratio, which is

a measure of the relative importance of the thermal to the ordinary diffusion, can be written as [44]

$$K_j^T = \frac{1}{5k_B N^2} \sum_k \frac{(6C^*_{jk} - 5)}{D_{jk}} \left(\frac{n_j M_j a_k - n_k M_k a_j}{M_j + M_k} \right) \qquad (38)$$

where a_j is the contribution of the j^{th} species to the mixture thermal conductivity (assuming that the internal degrees of freedom are frozen):

$$a_j = \lambda_j^0 \left[1 + \frac{1.065}{2\sqrt{2} n_j} \sum_{k \neq j} n_k C^*_{jk} \right]^{-1}, \qquad (39)$$

and C^*_{jk} is a ratio of collision integrals

$$C^*_{jk} = \frac{\Omega^{(1,2)*}_{jk}}{\Omega^{(1,1)*}_{jk}} . \qquad (40)$$

The expression for K^T_j has been derived by assuming that the gases in the mixture are monatomic or that the internal degrees of freedom are frozen. However, Chapman and Cowling [44] have conjectured that the internal degrees of freedom of the gas molecules is expected to have a smaller effect on the thermal diffusion ratio than on the thermal conductivity.

4.1.4 Chemical Kinetics

The chemical kinetic rate scheme is very specific for the problem being solved and the scheme [50] used for the hydrogen-oxygen-nitrogen system is presented later. The reaction rate constants are expressed in the modified-Arrhenius form:

$$k(T) = AT^B \exp(C/T) \qquad (41)$$

where T is the temperature (^oK) and A, B and C are constants.

4.1.5 Enthalpy and Specific Heats

The enthalpy of each species is expressed as

$$H_j = h_{oj} + h_j(T) \qquad (4-2)$$

where h_{oj} is the heat of formation of species j at 0^oK and h_j is the temperature dependent (sensible) enthalpy. These are available for a wide variety of species in the JANAF tables [51]. For computational convenience, the temperature dependent enthalpy has been fit to a power series in temperature as

$$h_j(T) = h_{j1} + h_{j2}T + h_{j3}T^2 + \ldots + h_{j7}T^6 . \qquad (4-3)$$

The specific heat at constant pressure for each of the species j is calculated from their enthalpies h_j by

$$C_{pj} = \left(\frac{dh_j}{dT}\right)_p \qquad (4-4)$$

4.2 Input Parameters for the Hydrogen-Oxygen-Nitrogen System.

The chemical kinetic rate scheme [50] used involves the eight reactive species H_2, O_2, O, H, OH, HO_2, H_2O_2, H_2O and diluent which is considered to be N_2. The reaction scheme and the constants in the reaction rate expression (Eq. 4-1) are presented in Table I. This scheme has been extensively tested against experimental data [50,52] and shown to give good results. Burks and Oran [50] showed that the results computed with this scheme compared very well with experimentally observed induction times, second explosion limits and the temporal behavior of reactive species. Oran, et al. [52] have shown that the scheme gives good results when coupled with a fluid dynamic model in the simulation of the conditions behind a reflected shock.

Table I. H_2–O_2 Elementary Reactive Mechanism

Reaction	$k_f = AT^B \exp(-C/T)$[a] A[b]	B	C[b]	References
$H + HO \rightleftharpoons O + H_2$	1.40(-14)	1.00	3.50(+03)	[56]
	3.00(-14)	1.00	4.48(+03)	[56]
$H + HO_2 \rightleftharpoons H_2 + O_2$	4.20(-11)	0.00	3.50(+02)	[56]
	9.10(-11)	0.00	2.91(+04)	[56]
$H + HO_2 \rightleftharpoons HO + HO$	4.20(-10)	0.00	9.50(+02)	[56]
	2.00(-11)	0.00	2.02(+04)	[56]
$H + HO_2 \rightleftharpoons O + H_2O$	8.30(-11)	0.00	5.00(+02)	[57]
	1.75(-12)	0.45	2.84(+04)	$k_r = k_f/K_c$
$H + H_2O_2 \rightleftharpoons HO_2 + H_2$	2.80(-12)	0.00	1.90(+03)	[56]
	1.20(-12)	0.00	9.40(+03)	[56]
$H + H_2O_2 \rightleftharpoons HO + H_2O$	5.28(-10)	0.00	4.50(+03)	[56]
	3.99(-10)	0.00	4.05(+04)	$k_r = k_f/K_c$
$HO + H_2 \rightleftharpoons H + H_2O$	1.83(-15)	1.30	1.84(+03)	[58]
	1.79(-14)	1.20	9.61(+03)	[58]
$HO + HO \rightleftharpoons H_2 + O_2$	1.09(-13)	0.26	1.47(+04)	$k_f = k_r/K_c$
	2.82(-11)	0.00	2.42(+04)	[59]
$HO + HO \rightleftharpoons O + H_2O$	1.00(-16)	1.30	0.00(+00)	[58]
	3.20(-15)	1.16	8.77(+03)	$k_r = k_f/K_c$
$HO + HO_2 \rightleftharpoons H_2O + O_2$	8.30(-11)	0.00	5.03(+02)	[60]
	2.38(-10)	0.17	3.69(+04)	$k_r = k_f/K_c$
$HO + H_2O \rightleftharpoons HO_2 + H_2$	1.70(-11)	0.00	9.10(+02)	[56]
	4.70(-11)	0.00	1.65(+04)	[56]
$HO + H_2 \rightleftharpoons HO + H_2O$	1.20(-12)	0.00	9.41(+03)	[59]
	1.33(-14)	0.43	3.62(+04)	$k_r = k_f/K_c$
$HO_2 + HO_2 \rightleftharpoons H_2O_2 + O_2$	3.00(-11)	0.00	5.00(+02)	[57]
	1.57(-09)	-0.38	2.20(+04)	$k_r = k_f/K_c$

Table I. H_2-O_2 Elementary Reactive Mechanism
(Continued)

Reaction	$k_f = AT^B \exp(-C/T)$[a] A[b]	B	C[b]	References
$O + HO \rightleftharpoons H + O_2$	2.72(-12)	0.29	-8.10(+01)	$k_r = k_f/K_c$
	3.70(-10)	0.00	8.45(+03)	[56]
$O + HO_2 \rightleftharpoons HO + O_2$	5.32(-11)	0.00	5.03(+02)	[60]
	2.20(-11)	0.19	2.82(+04)	$k_r = k_f/K_c$
$O + H_2O_2 \rightleftharpoons H_2O + O_2$	1.40(-12)	0.00	2.12(+03)	[57]
	5.70(-14)	0.52	1.48(+04)	$k_r = k_f/K_c$
$O + H_2O_2 \rightleftharpoons HO + HO_2$	1.40(-12)	0.00	2.13(+03)	[57]
	2.07(-15)	0.64	8.23(+03)	$k_r = k_f/K_c$
$H + H + M \rightleftharpoons H_2 + M$	1.80(-30)	-1.00	0.00(+00)	[56]
	3.70(-10)	0.00	4.83(-04)	[56]
$H + HO + M \rightleftharpoons H_2O + M$	6.20(-26)	-2.00	0.00(+00)	[56]
	5.80(-09)	0.00	5.29(+04)	[56]
$H + O_2 + M \rightleftharpoons HO_2 + M$	4.14(-33)	0.00	-5.00(+02)	[56]
	3.50(-09)	0.00	2.30(+04)	[56]
$HO + HO + M \rightleftharpoons H_2O_2 + M$	2.60(-33)	0.00	-2.55(+03)	[56]
	2.00(-07)	0.00	2.29(+04)	[56]
$O + H + M \rightleftharpoons HO + M$	9.28(-29)	-1.00	0.00(+00)	[61]
	2.33(-10)	0.21	5.10(+04)	$k_r = k_f/K_c$
$O + HO + M \rightleftharpoons HO_2 + M$	2.80(-31)	0.00	0.00(+00)	[61]
	1.10(-04)	-0.43	3.22(+04)	$k_r = k_f \cdot K_c$
$O + O + M \rightleftharpoons O_2 + M$	5.20(-35)	0.00	-9.00(+02)	[56]
	3.00(-06)	-1.00	5.94(+04)	[56]

(a) Bimolecular reaction rate constants are given in units of $cm^3/(molecule\ sec)$. Termolecular reaction rate constants are given in units of $cm^6/(molecule^2\ sec)$.
(b) Exponentials to the base 10 are given in parenthesis; i.e., 1.00(-10) = 1.00×10^{-10}.

For the calculation of the thermal conductivity, the binary diffusion coefficients and the thermal diffusion ratios, we need the collision integrals $\Omega^{(1,1)*}$, $\Omega^{(1,2)*}$ and $\Omega^{(2,2)*}$. These depend on the intermolecular potential function chosen. For the results presented in the next section, we have used the Lennard-Jones (6-12) potential function which adequately describes the interaction of non-polar molecules. This potential function can be written as

$$\phi(r) = 4\varepsilon\left[\left(\frac{\sigma}{r}\right)^{12} - \left(\frac{\sigma}{r}\right)^{6}\right] \qquad (45)$$

where ε is the depth of the potential well (the maximum energy of attraction) and σ is the collision diameter for low energy collisions. The collision integrals for this potential function have been calculated and tabulated in many independent investigations (e.g. Ref. [46], [53]). We have used the tabulations of Klein et al [53]. There is some uncertainty in the values of the parameters σ and ε in Eq. (45). The parameters we have used are presented in Table II and, except for σ_H, σ_{H_2O} and ε_{H_2O} are those given by Svehla [54]. Since H_2O is a polar molecule the Lennard-Jones potential function is a poor approximation. A Stockmayer-type potential function may be more applicable to polar molecules [54]. However we have assumed that the Lennard-Jones potential function is valid for H_2O, but have used the values given by Dixon-Lewis [33] for σ_{H_2O} and ε_{H_2O} (and for σ_H) which he has found to be satisfactory in extensive investigations of the H_2-O_2 system.

The ordinary diffusion coefficients have been calculated using Eq. (33), where the values of A_{jk} and B_{jk} have been taken from the data given by Mason and Marrero [49]. However, no such data is available for many pairs

Table II. Lennard-Jones (12:6) Potential Parameters

Species	ϵ/k (^0K)	$\sigma(10^{-8}$ cm)
H	37	3.5
O	106.7	3.05
H_2	59.7	2.827
OH	79.8	3.147
H_2O	260.0	2.8
O_2	106.7	3.467
HO_2	106.7	3.467
H_2O_2	289.3	4.196
N_2	71.4	3.798

of species occurring in the hydrogen-oxygen-nitrogen system. For these pairs of species the diffusion coefficients have been estimated by noting from Eq. (3-) that if two pairs of species (j,k) and (l,m) have similar values for the $\Omega^{(1,1)*}$ term, then their binary diffusion coeffients can be related by

$$\frac{D_{jk}}{D_{lm}} = \frac{\sigma_{lm}^2}{\sigma_{jk}^2} \left[\frac{\mu_{lm}}{\mu_{jk}}\right]^{1/2} \tag{46}$$

where

$$\mu_{jk} = \frac{M_j M_k}{M_j + M_k} \tag{47}$$

and

$$\sigma_{jk} = \frac{\sigma_j + \sigma_k}{2} \quad . \tag{48}$$

However, this procedure only modifies the temperature-independent term A_{jk}. When $\Omega^{(1,1)*}$ for the two pairs of species is very different the temperature dependence (and hence B_{jk}) will also have to be modified. The values for A_{jk} and B_{jk} for all the pairs of species occurring in the hydrogen-oxygen-nitrogen system are presented in Table III. Using Eq. (33) rather than Eq. (34) avoids using tables to evaluate the collision integral $\Omega_{jk}^{(1,1)*}$ for each pair of species at each temperature.

For the thermal diffusion ratio (Eq. 38), the ratio of collison integrals C_{jk}^* has been assumed to be unity. Although the collision integrals $\Omega^{(1,1)*}$ and $\Omega^{(1,2)*}$ are different from unity and vary with temperature, their ratio is close to unity and hardly varies with temperature. The collision integrals and their ratio for a range of temperatures (300K - 3000K) for the $H-N_2$ pair is given in Table IV.

Table III. Binary Diffusion Coefficients expressed in the form: $D_{jk} = A_{jk} T^{B_{jk}}/N$

Species	O	H_2	OH	H_2O	O_2	HO_2	H_2O_2	N_2
H	6.30(+17) 7.28(-01)	8.29(+17) 7.28(-01)	6.30(+17) 7.28(-01)	6.70(+17) 7.28(-01)	6.70(+17) 7.32(-01)	6.70(+17) 7.32(-01)	4.43(+17) 7.28(-01)	6.10(+17) 7.32(-01)
O		3.61(+17) 7.32(-01)	1.22(+17) 7.74(-01)	2.73(+17) 6.32(-01)	9.69(+16) 7.74(-01)	9.69(+16) 7.74(-01)	1.57(+17) 6.32(-01)	9.69(+16) 7.74(-01)
H_2			3.49(+17) 7.32(-01)	6.41(+17) 6.32(-01)	3.06(+17) 7.32(-01)	3.06(+17) 7.32(-01)	4.02(+17) 6.32(-01)	2.84(+17) 7.38(-01)
OH				2.73(+17) 6.32(-01)	1.16(+17) 7.24(-01)	9.69(+16) 7.74(-01)	1.57(+17) 6.32(-01)	9.69(+16) 7.74(-01)
H_2O					2.04(+17) 6.32(-01)	2.04(+17) 6.32(-01)	1.57(+17) 6.32(-01)	1.89(+17) 6.32(-01)
O_2						8.74(+16) 7.24(-01)	1.14(+17) 6.32(-01)	8.29(+16) 7.24(-01)
HO_2							1.14(+17) 6.32(-01)	8.25(+16) 7.24(-01)
H_2O_2								1.14(+17) 6.32(-01)

Note: For each pair of species, the upper term is A_{jk} and the lower term is B_{jk}; e.g. $D_{H-O} = 6.3 \times 10^{17} T^{0.728}/N$.

Table IV. The Ratio C^*_{jk} as a Function of the Reduced Temperature T* for H-N_2

T(°K)	T^*	$\Omega^{(1,2)*}_{jk}$	$\Omega^{(1,2)}_{jk}$	C^*_{jk}
300	5.837	0.76458	0.81740	0.9354
500	9.728	0.70387	0.74570	0.9439
1000	19.456	0.63215	0.66696	0.9478
2000	38.912	0.56789	0.59886	0.9483
3000	58.368	0.53309	0.56233	0.9480

5. IGNITION, QUENCHING AND PROPAGATION OF FLAMES IN HYDROGEN-OXYGEN-NITROGEN MIXTURES.

The model described above has been used to study a variety of problems. These include the calibration of a theoretical model for the ignition of premixed gases [6,7], calculations of flammability limits [8] and the estimation of burning velocities [9]. In this section we first discuss some of the results obtained in a study of the ignition and quenching of a $2{:}1{:}10/H_2{:}O_2{:}N_2$ mixture [7]. This is an inherently time-dependent problem and we can take advantage of this property of the model. The second problem discussed is a simulation of a propagating flame in a stoichiometric H_2-air mixture. The steady state burning velocity, that is, the velocity of the flame relative to that of the unburned gases, has been estimated from the time-dependent simulations. In both cases, the initial temperatures and pressures of the unburned gases were 298K and 1 atm, respectively.

5.1 Minimum Ignition Energies and Quenching Distances

The model was configured in spherical geometry with an open boundary at one end to simulate a very large system. Energy was deposited at the center with a radius of deposition, R_c. Results from a typical calculation are presented in Fig. 1. The figure depicts the time history of the temperature profile after 4 mJ of energy is deposited linearly over a period of 0.1 ms. Even after the energy deposition is stopped, the central temperature continues to increase due to the heat released in chemical reactions. With time, however, the temperature near the center decreases and the temperature away from the center increases due to diffusive transport. By 4.5 ms, we see that the temperature distribution exhibits a "flame" temperature profile.

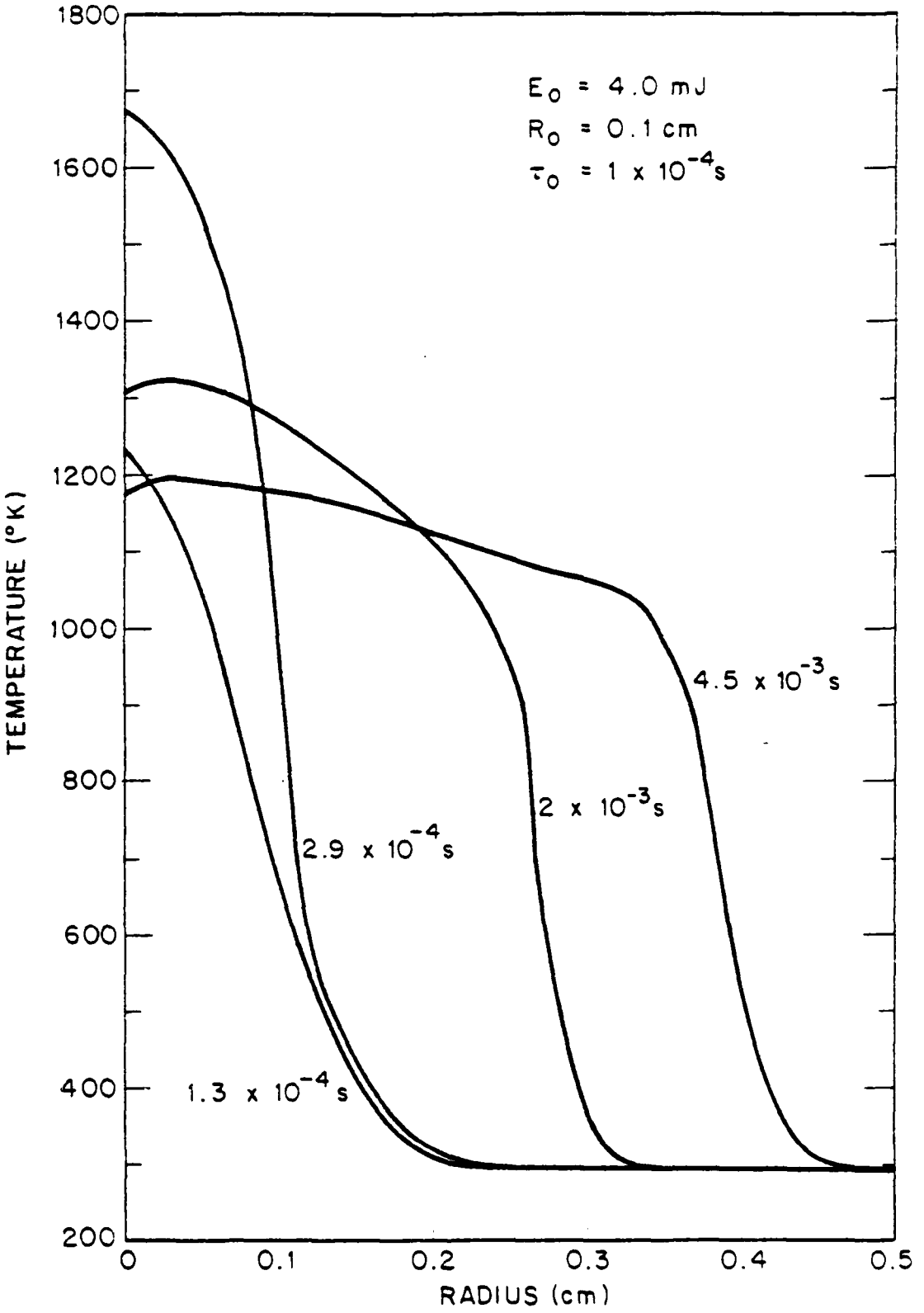

Fig. 1 — Time history of the temperature profile in a H_2:O_2:N_2:2:1:10 mixture

When the amount of energy deposited, E_o, was reduced to 3 mJ, the temperature distribution did not develop into a flame temperature profile.

By repeating the computations for different values of E_o, a bound for the minimum ignition energy for that particular radius was obtained. Similar calculations were performed for different values of the radius of deposition, R_o. The results of such investigations are shown in Fig 2. A propagating flame results when 3.6 mJ of energy is deposited in a sphere with a radius of 0.1 cm. However if the same amount of energy is deposited in a sphere of smaller radius, the rate of heat liberation is insufficient to compensate for the rate of heat loss and consequently there is no ignition. This radius, 0.1 cm, is the "quench-radius" for this particular mixture. For radii slightly larger than the quench-radius, the minimum ignition energy is almost constant and for larger radii (larger than 0.11 cm) the minimum ignition energy increases rapidly with increasing radii. Therefore for the system under study, the absolute minimum energy is about 3.7 mJ. These observations are in qualitative agreement with those of Lewis and von Elbe [55]. Quantitative comparisons are not possible since the composition of the mixture and the time for energy deposition are different.

5.2 Flame Propagation in Stoichiometric H_2-Air Mixtures at 298K and 1 atm.

The model described above can also be used to study the propagation of flames in premixed gases. As shown in Fig. 1, if sufficient energy is deposited at the center of a sphere and computations are carried out for a sufficiently long time, the temperature distribution attains a typical "flame profile". However, this method is an expensive way to generate a propagating flame since so much time is spent in establishing and overcoming the initial conditions. Another method for initializing the problem quickly is to start

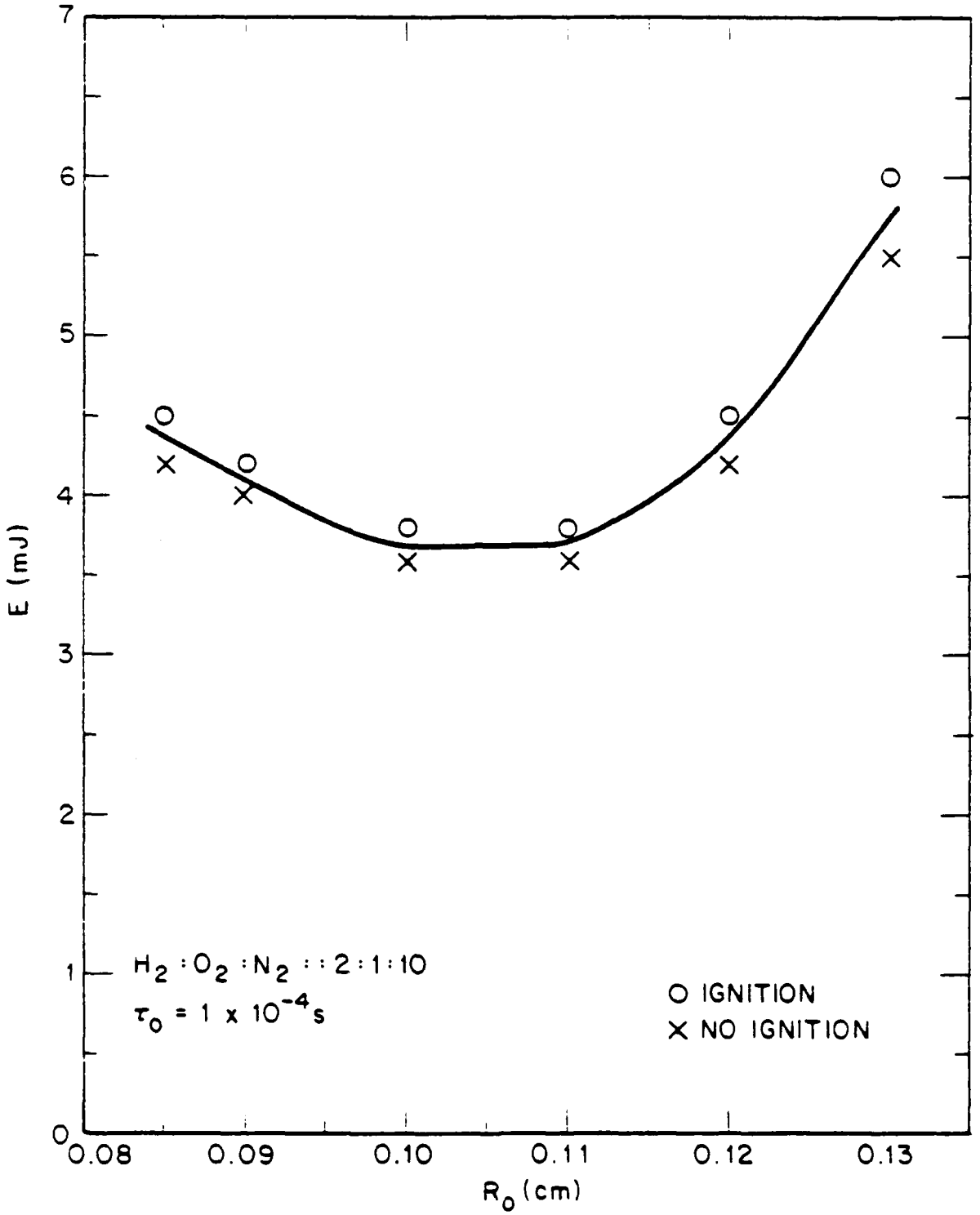

Fig. 2 — The minimum ignition energy as a function of the radius of energy deposition

the computations with a good guess for the temperature and species profile in a region behind a flame front. The closer the initial profiles are to the final, steady state flame profile, the sooner the initial conditions relax to the steady propagating flame.

For the results discussed below, the model was set up in Cartesian geometry with one end closed (preventing any gas flow through it) and the other open to the atmosphere. At the closed end, a first approximation to the temperature and major species profile was set up as initial conditions.

In order to evaluate the importance of the thermal diffusion in the propagation of flames we have studied two cases. For the first case the effects of thermal diffusion have not been considered, that is the source terms due to thermal diffusion in Eq. (8) have been neglected. For case 2, the thermal diffusion ratio K_j^T of all species have been calculated using Eq. (38). However, in both cases the heat flux due to concentration gradients (the Dufour effect) has not been considered since it is expect to be negligible even when thermal diffusion is not negligible [10].

Case 1: Thermal Diffusion Neglected.

The calculations were initialized as described above and soon a propagating flame developed as can be seen in Fig. 3, where the temperature profiles at 15 μs and 20 μs (from the start of the computations) are shown. In order to determine the flame speed, a criterion for the location of the flame is required since the flame is of finite thickness. One method is to choose an arbitrary value of temperature in the high gradient region to define the location of the flame. The movement of the location of this value in time and space gives the rate of propagation of the flame. The location of the flame (defined by 900 K) is presented as a function of time in Fig. 4. The

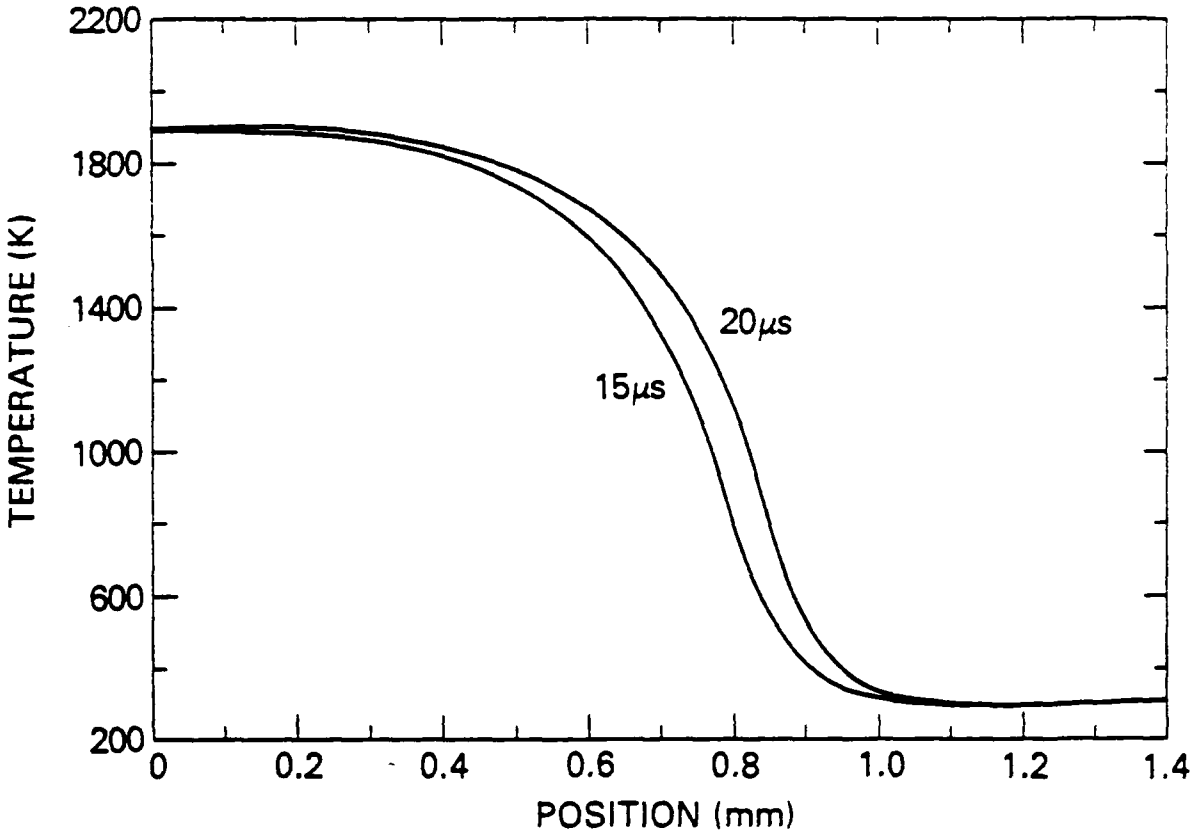

Fig. 3 — Temperature profiles in a propagating flame

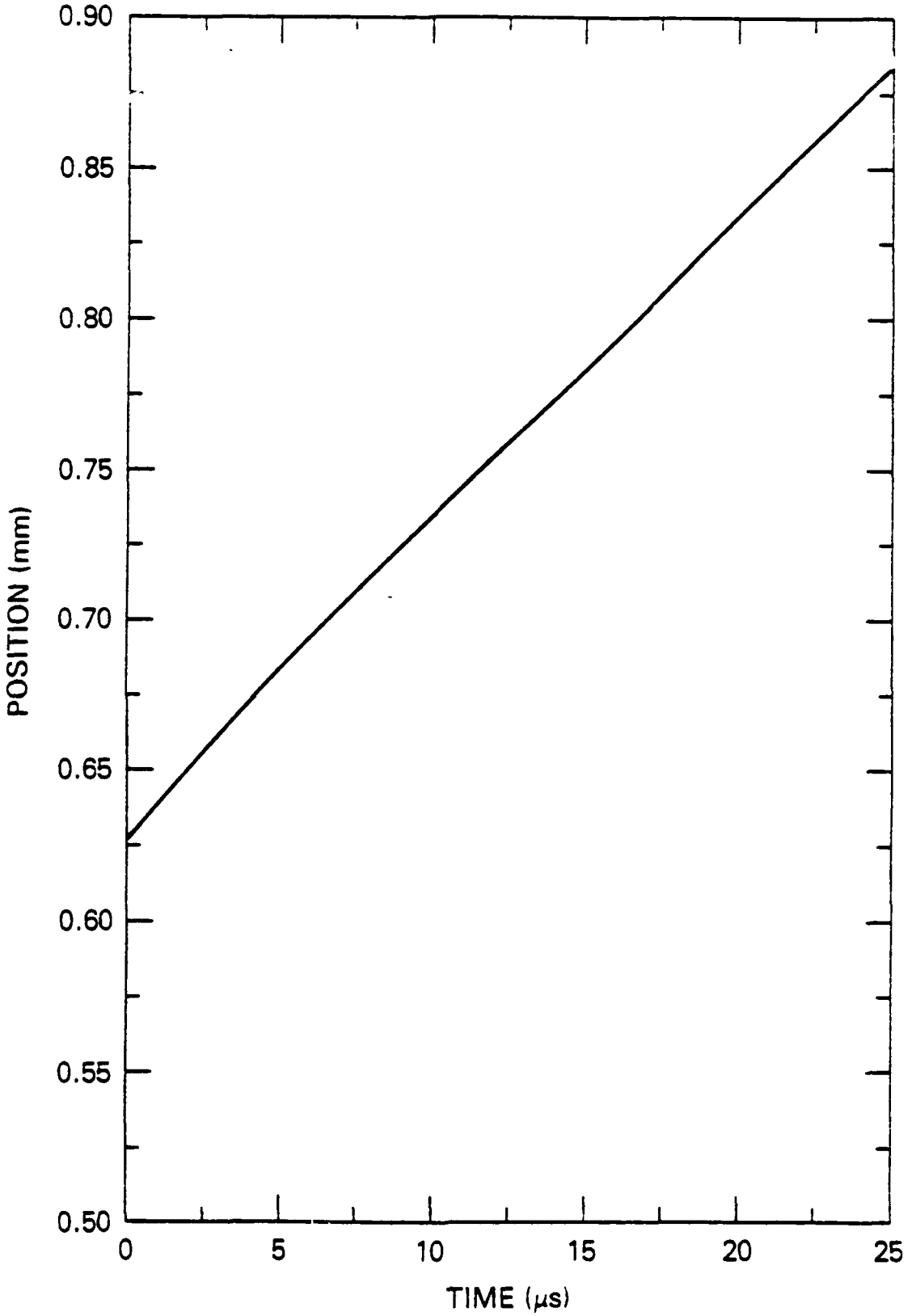

Fig. 4 — Time history of the location of a flame in a stoichiometric hydrogen-air mixture

slope of this curve gives the flame velocity for an inertial observer and it is shown as curve 'a' in Fig. 5. The flame propagates initially at a velocity of about 11 m/s but by 20 μs (from the start of the computations) it attains a nearly constant value of 10 m/s.

A quantity of considerable practical interest is the burning velocity which is defined as the rate at which the flame consumes the reactants, or equally well as the velocity of the flame relative to that of the unburned gases. In Fig. 6 the fluid velocity profile in the system is depicted at a particular time. The velocity is zero at one end since that end is a closed boundary. The flow velocity increases across the flame and is maximum at the open boundary. An estimate for the burning velocity can be obtained by subtracting the velocity of the unburned gases from the flame velocity. However, there is some uncertainty in the evaluation of the velocity of the unburned gases since the location of the flame front itself is arbitrary. The temperature profile across the system has also been depicted in Fig. 6. From this figure we see that an upper estimate for the velocity of the unburned gases is the fluid velocity at the open boundary. The flow velocity at the open-boundary (which is also the rate of movement of the open boundary because of the Lagrangian coordinate system used) is shown in Fig. 5 as curve (b). Corresponding to the "steady" flame velocity of 10 m/s, the velocity of the unburned gases is about 7.85 m/s. This gives a burning velocity of 2.15 m/s for the stoichiometric hydrogen-air flame studied.

There are small oscillations in the flame velocity shown in Fig. 5(a) and these lead to uncertainties in the estimate of the "steady" flame velocity. The amplitude of the oscillations decreases when the spatial resolution is increased. This can be seen in Fig. 7 where the time history of the flame

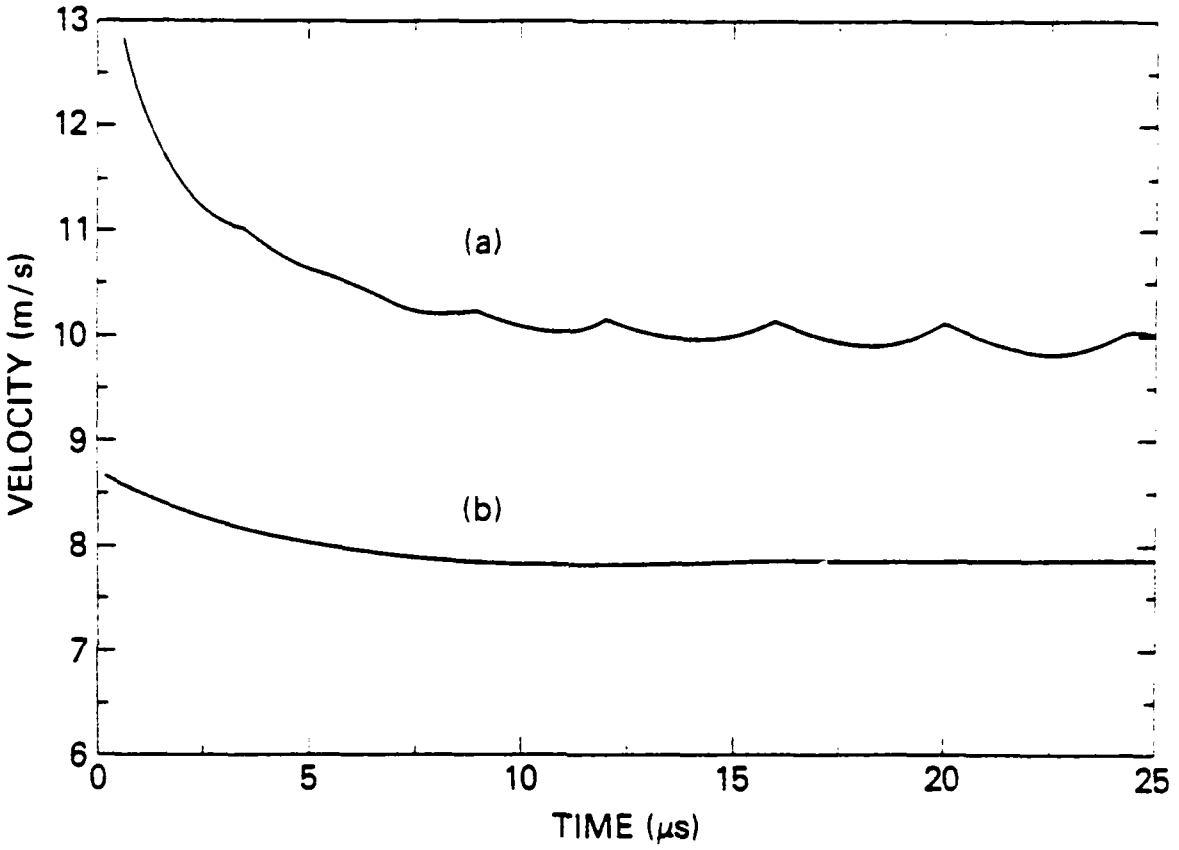

Fig. 5 — Time history of the velocity of (a) the flame and (b) the fluid at the open boundary

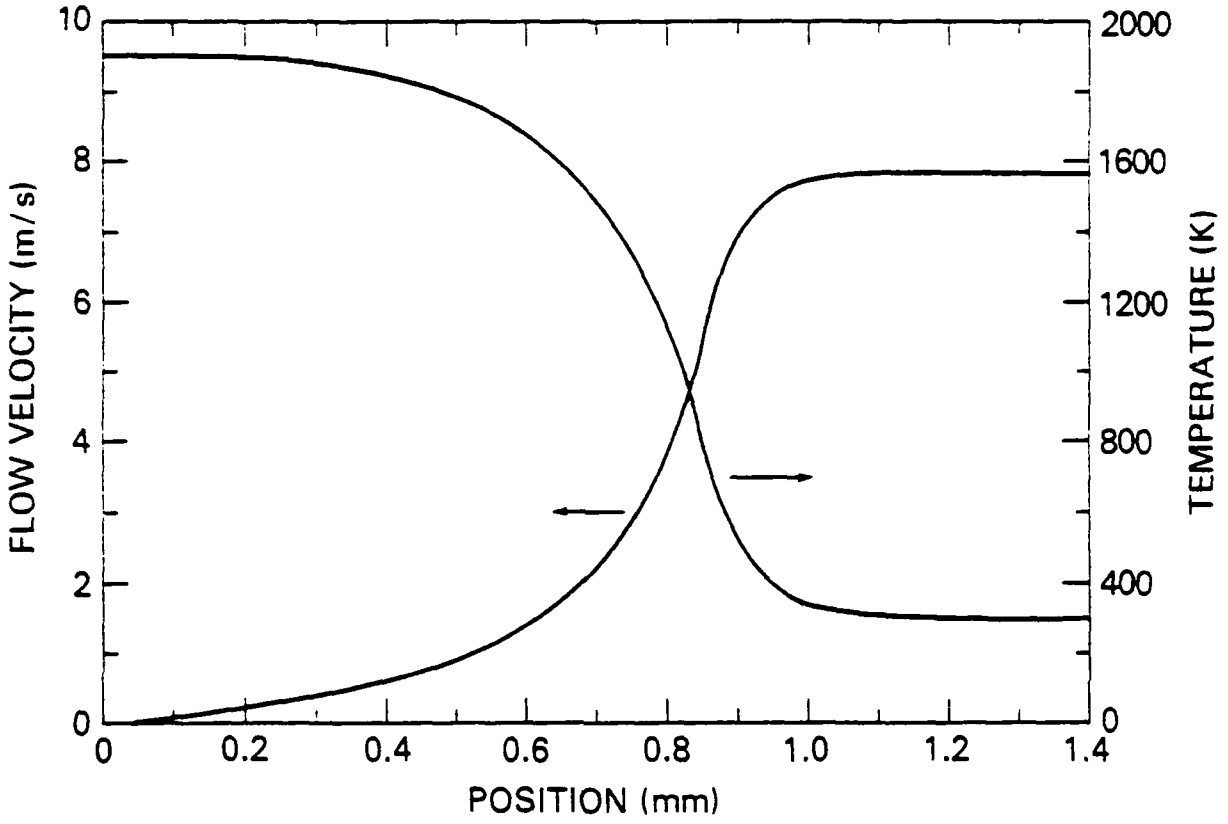

Fig. 6 — The flow velocity and temperature profiles in a propagating flame

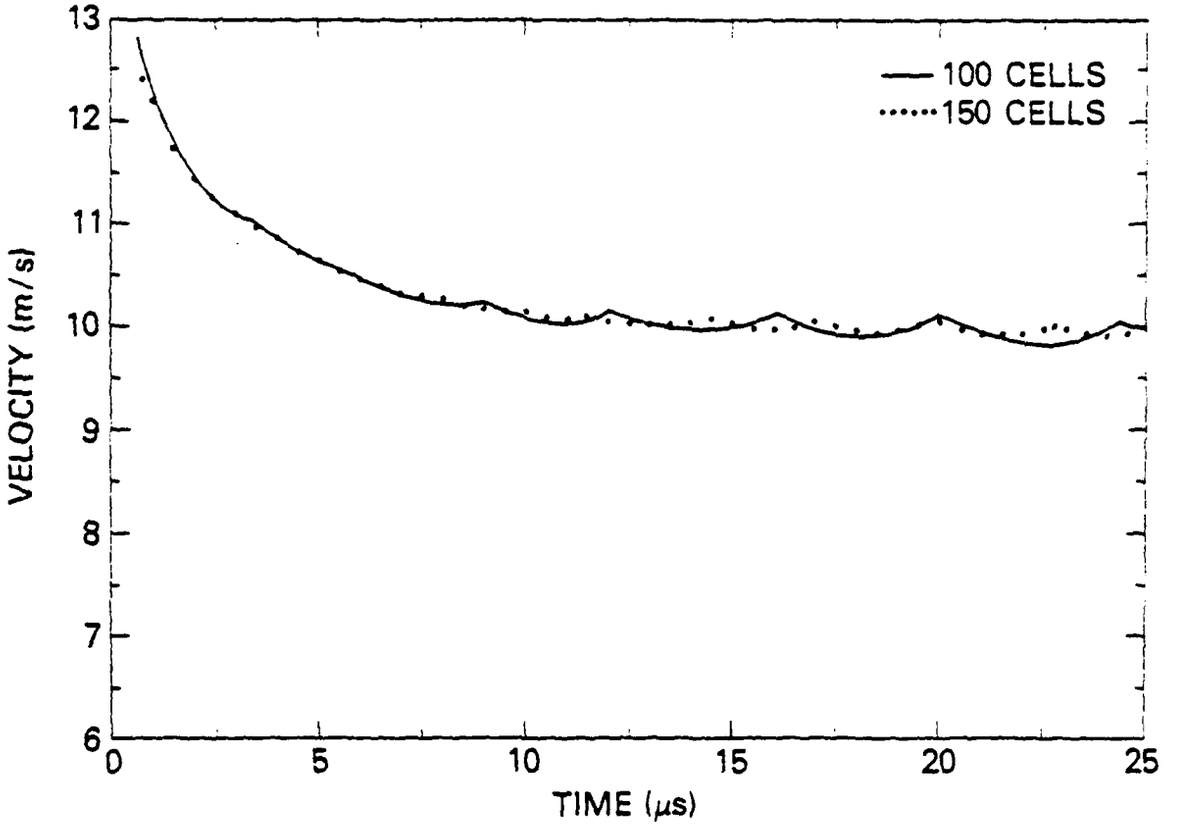

Fig. 7 — Effect of spatial resolution on the time history of the flame velocity

velocity computed using 100 grid points (cells) is compared to that using 150 grid points. Since the computations are initialized using the uniformly spaced grid, when the number of grid points is increased the spatial resolution increases all across the system even in the region well ahead of the flame front.

Case 2. Effect of Thermal Diffusion on Burning Velocity

In this case the thermal diffusion source terms in Eq. (8) were included in the calculation of the diffusion velocities. The flame velocity and the velocity of the unburned gases were determined as described above for case 1. The time history of these velocities have been compared to those of case 1 in Fig. 8. The effect of thermal diffusion is to reduce both the flame velocity and the velocity of the unburned gases. The "steady" flame velocity (corresponding to 20 μs from the start of the calculations) decreases from 10 m/s to about 9.65 m/s while the corresponding velocity of the unburned gases decreases from 7.85 m/s to about 7.65 m/s. The net effect is to lower the burning velocity of the stoichiometric hydrogen-air mixture to about 2 m/s. The reasons for these effects are examined below.

The source terms considered in Eq. (7) for the calculation of diffusion velocities are:

(a) due to concentration gradients (ordinary diffusion)

$$S_{OD} = \nabla\left(\frac{n_i}{N}\right) \tag{49}$$

(b) due to temperature gradients (thermal diffusion)

$$S_{TD} = K_j^T \frac{\nabla T}{T} . \tag{50}$$

The spatial variations of these two terms have been calculated for the steady

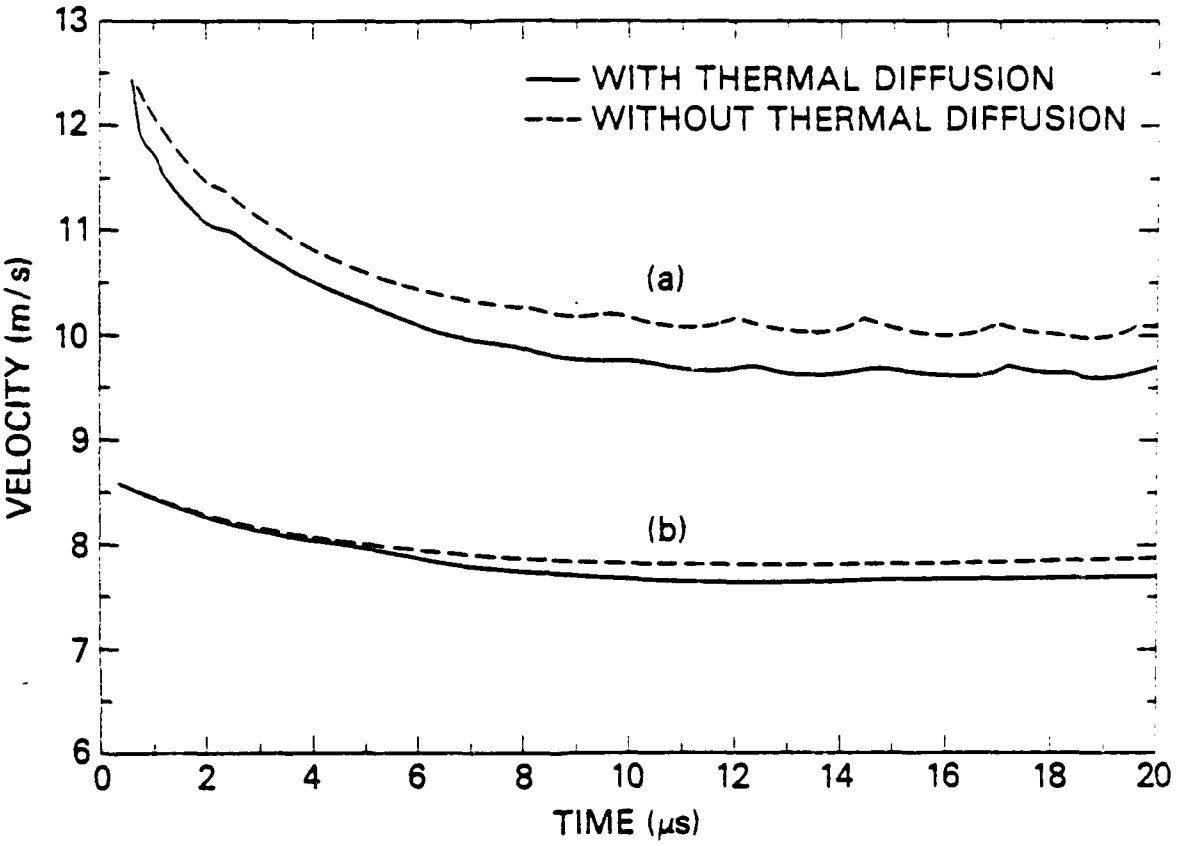

Fig. 8 — Effect of thermal diffusion on the time history of the velocity of (a) the flame and (b) the fluid at the open boundary

propagating flame coresponding to 20 μs in Fig. 8. The temperature profile across the system at 20 μs is given in Fig. 9. For convenience, the abscissa is given in cell numbers. In Fig. 9, the spatial variation of the source terms S_{OD} and S_{TD} have been compared for the species O_2 and N_2. We see that for O_2, the term S_{TD} is opposite in sign to S_{OD}. A negative value for S_{TD} implies that the oxygen molecules are diffusing from left to right, that is, from the hotter region to the cooler region. Since the sum of the two source terms determines the diffusion velocity, the effect of thermal diffusion is to slow the diffusion of oxygen molecules into the higher temperature region of the flame. The effect of this on the burning velocity is not obvious since it depends on the details of the reaction mechanism and the distribution of other radicals. For the species N_2, the term S_{TD} is comparable to the term S_{OD} and the effect of thermal diffusion is to enhance the movement of N_2 from the hotter region of the flame to the cooler region.

In Fig. 10, we compare the terms S_{OD} for the species H_2 and H. For H_2, the effect of thermal diffusion is similar to that of ordinary diffusion and it enhances the movement of H_2 from the cooler region to the hotter region. The term S_{OD} for the species H is particularly interesting. It is observed that the H atoms in the region up to cell number 75 (i.e. $T > 1400$ K have a tendency to diffuse into the hotter region while those after cell number 75 ($T < 1400$ K) diffuse into the cooler region. The diffusion of H atoms into the cooler region is very important in the propagation of the flame. The effect of thermal diffusion is to delay and decrease the diffusion of H atoms into the cooler region. Since the H atoms are produced primarily in the high temperature region (in fact here the concentration of H

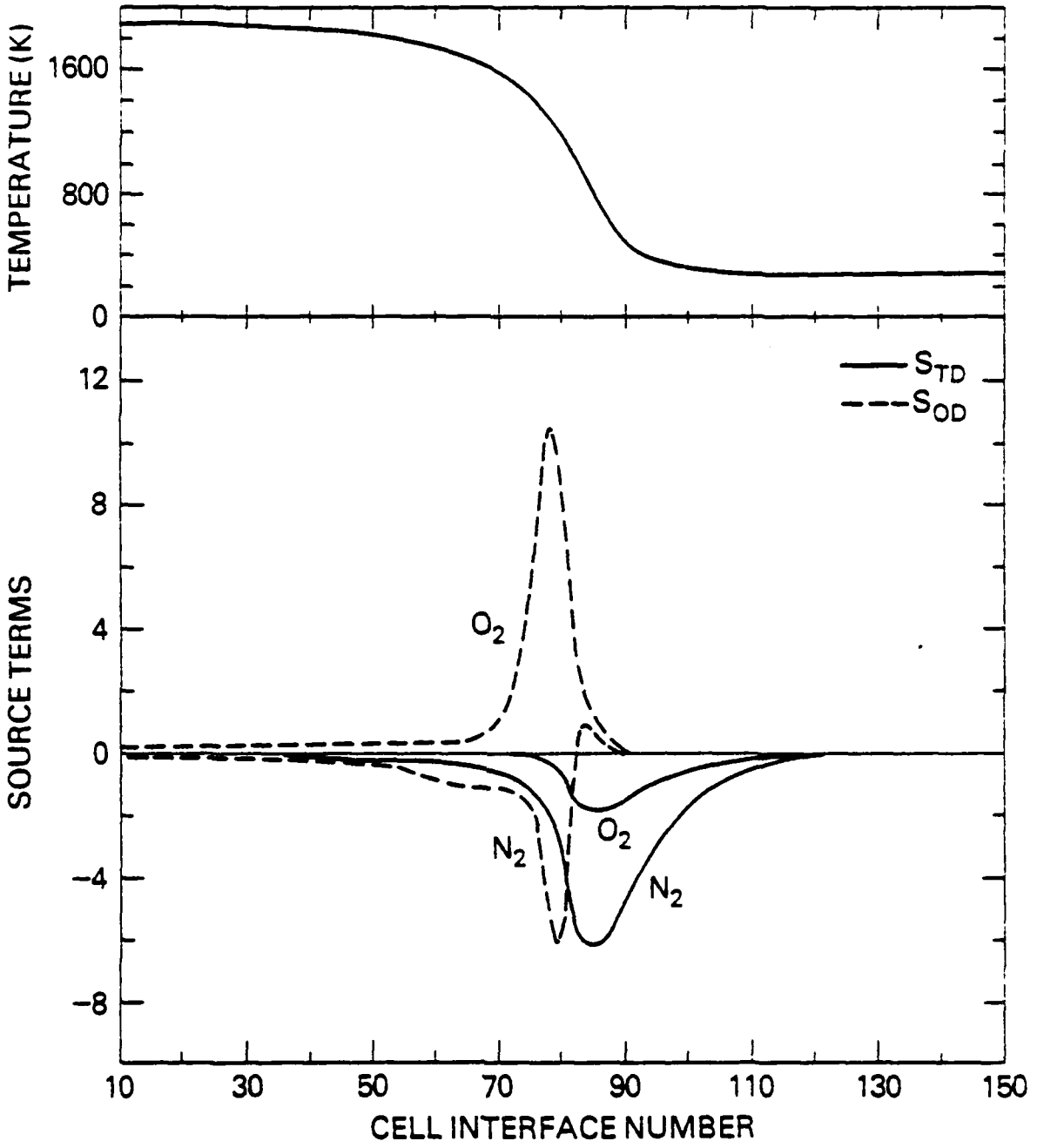

Fig. 9 — Comparison of the spatial variation of the source terms due to ordinary diffusion (S_{OD}) and thermal diffusion (S_{TD}) for the species O_2 and N_2. The temperature profile across the system has also been depicted.

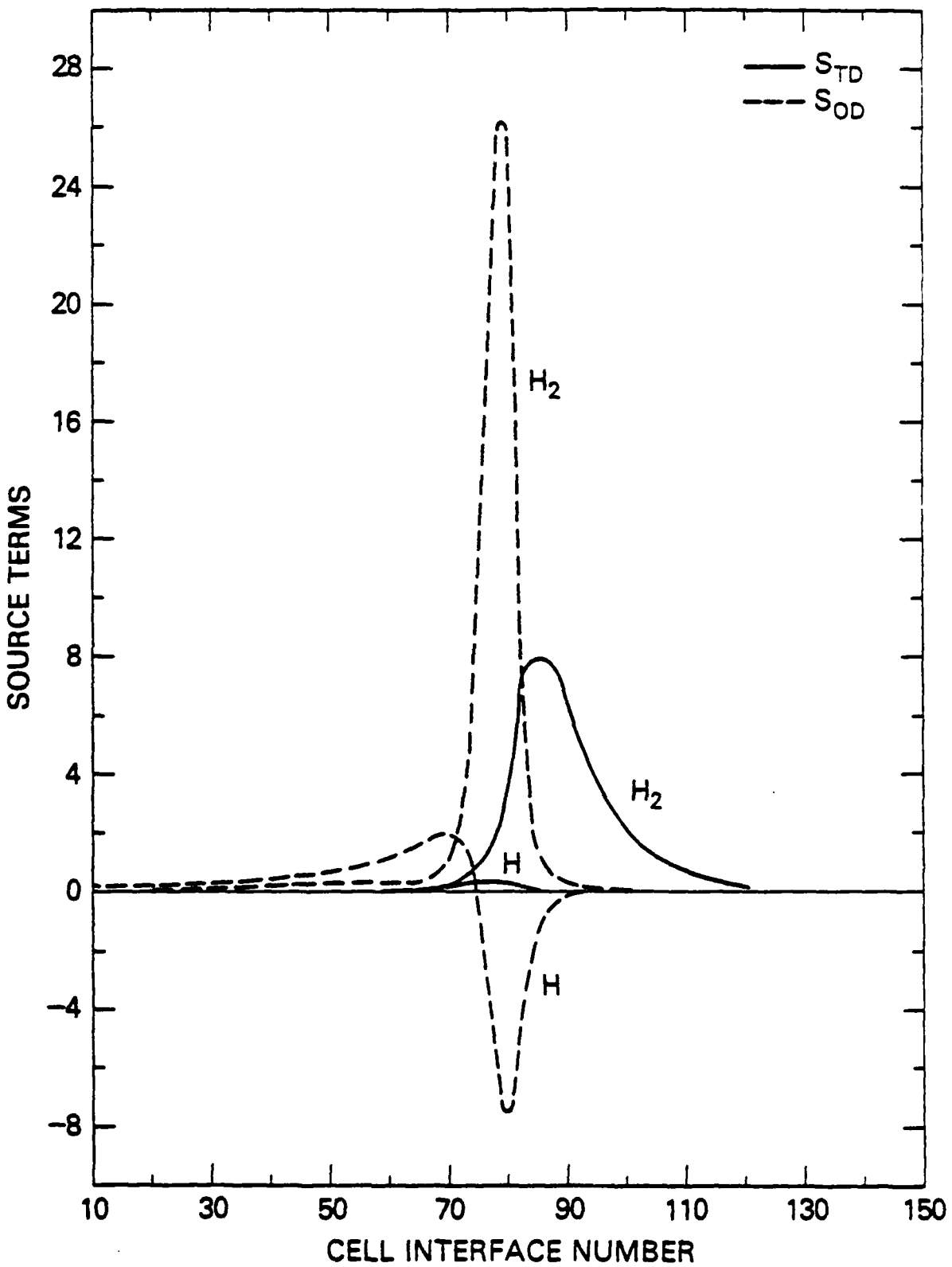

Fig. 10 — Comparison of the spatial variation of the source terms due to ordinary diffusion (S_{OD}) and thermal diffusion (S_{TD}) for the species H and H_2

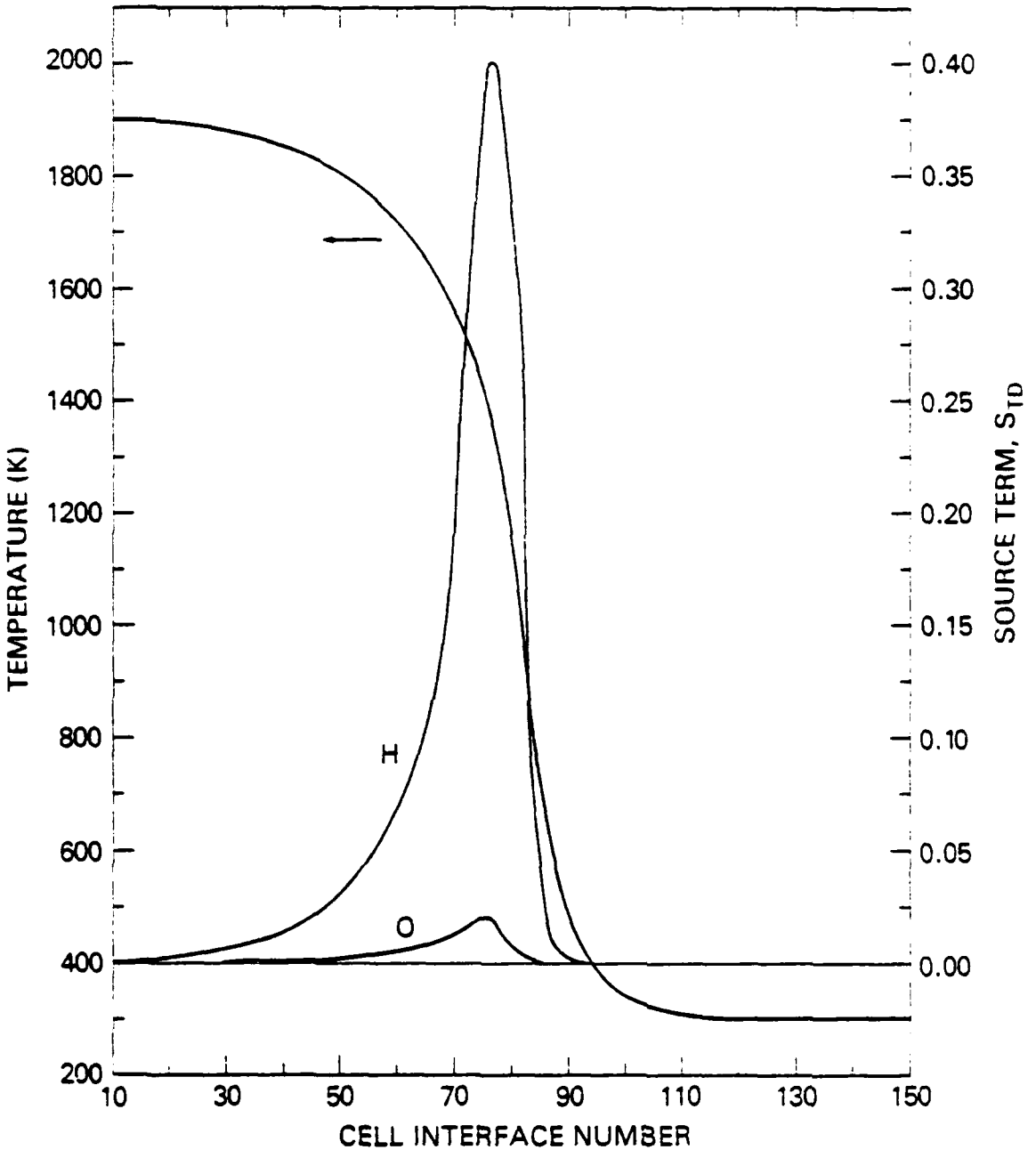

Fig. 11 — Comparison of the spatial variation of the thermal diffusion source term for the species H and O. The temperature profile across the system has also been depicted.

attains its maximum at cell number 75), thermal diffusion of H can significantly retard the rate of propagation of the flame. This may be the main reason for the observed reduction in the burning velocity when the effects of thermal diffusion were included.

The term S_{TD} for the other species in the system is small compared to the term S_{OD}. In Fig. 11 we also see that the source term due to thermal diffusion of oxygen atoms is significantly less than that due to hydrogen atoms.

6. SUMMARY AND CONCLUSIONS

This report described a one-dimensional, time-dependent, Lagrangian model for predicting the initiation, propagation and quenching of laminar flames in pre-mixed gases. A number of new approaches and algorithms used in the model have been discussed. An asymptotic coupling method was used in conjunction with timestep splitting to couple the various physical and chemical processes. This approach allowed the use of entirely different algorithms for the processes represented by different terms in the conservation equations. This made the computing procedure very efficient and inexpensive.

The result from several calculations using the model have been presented. The first is a flame initiation and minimum ignition energy study of a hydrogen, oxygen, nitrogen mixture. This used the time-dependent property of the model and the obervations were in qualitative agreement with experimental data. Quantitative comparisons were not possible since the composition of the mixture and the time for energy deposition were different. The second problem discussed was an estimation of the steady state burning velocity of a stoichiometric hydrogen-air mixture. The burning velocity predicted by the model was on the lower end of the observed experimental range. We note, however, that there are several factors which would tend to increase this estimated value. First, the calculated burning velocity would be larger if the velocity of the unburned gas used in this calculation was closer to the flame front instead of at the open boundary. It is not clear where it should be evaluated in a time-dependent calculation. Second, the uncertainties in the values of some of the diffusion coefficients are about 30%. The

burning velocity was found to be very sensitive to certain diffusion coefficients. Because of the uncertainty in the experimental values of the diffusion coefficients, there may not be any advantage in using the empirical formula over the expression from kinetic theory.

The model also predicts that the effect of thermal diffusion is to lower the burning velocity by about 7%. This observation is in agreement with that of Dixon-Lewis [32] who found that neglecting thermal diffusion of hydrogen atoms increases the burning velocity by 5 or 6%. For the hydrogen atom, the thermal diffusion source term was found to be small compared to the source term due to ordinary (concentration) diffusion. But because of the complex chemistry occurring in flames, a small difference in the hydrogen source term causes a significant difference in the burning velocity. This again emphasizes the need for more accurate estimates of the diffusion coefficients.

In conclusion, the model can be used confidently to predict the ignition, propagation and quenching of laminar flames in pre-mixed gases provided there is satisfactory data on the chemical kinetics and the diffusive transport coefficients.

ACKNOWLEDGMENTS

The authors would like to acknowledge the help and advice of T.R. Young, J.M. Picone, and Homer Carhart. This work is sponsored by the Office of Naval Research and the Naval Material Command.

REFERENCES

1. Boris, J.P., ADINC: An Implicit Lagrangian Hydrodynamics Code, NRL Memorandum Report 4022, Naval Research Laboratory, Washington, DC, 1979

2. Oran, E.S., and Boris, J.P., Prog. Energy Combustion Science, 7:1-72 (1981).

3. Jones, W.W., and Boris, J.P., Comp. Chem. 5, 139-146 (1981).

4. Young, T.R., and Boris, J.P., J. Phys. Chem. 81, 2424-2427 (1977).

5. Young, T.R., CHEMEQ - A Subroutine for Solving Stiff Ordinary Differential Equations, NRL Memorandum Report 4091, Naval Research Laboratory, Washington, DC, 1980.

6. Oran, E.A., and Boris, J.P., presented at the 7th International Colloquium on Gas Dynamics of Explosions and Reactive System, Göttingen, 1979, appears in Prog. in Astronautics and Aeronautics, 76:154-171 (1981).

7. Kailasanath, K., Oran, E.S., and Boris J.P., A Theoretical Study of the Ignition of Pre-Mixed Gases, 1982 (to appear in Combust. Flame).

8. Indritz, D., Boris, J., Carhart, H., Oran, E., Sheinson, R., Williams, F., and Young, T., Computation of Hydrogen-Oxygen Flammability Limits, submitted to Comb. Flame.

9. Kailasanath, K., Oran, E.S., Boris, J.P., and Young, T.R., Time-Dependent Simulation of Flames in Hydrogen-Oxygen-Nitrogen Mixtures, to appear in the Proceedings of the GAMM Workshop on Numerical Methods in Laminar Flame Propagation, Vieweg-Verlag, W. Germany, 1982.

10. Williams, F.A., Combustion Theory, Addison Wesley, Reading, MA, 1965, p. 2.

11. Mallard, E., and LeChatelier, H.L., Ann. Mines 4, 379 (1883).

12. von Karman, T., and Penner, S.S., Selected Combustion Problems, Fundamentals and Aeronautical Applications, AGARD, Butterworths Scientific Publications, London, 5-41 (1954); von Karman, T., Sixth Symposium (International) on Combustion, Reinhold Publishing Co., New York, pp. 1-11 (1957).

13. Zeldovich, Y.B., and Frank-Kamenetski, D.A., J. Phys. Chem. (USSR) 12, 100 (1938); Zeldovich, Y.B., and Semenov, N.N., J. Exptl. Theoret. Phys. (USSR) 10, 1116 (1940); Zeldovich, Y.B., J. Phys. Chem (USSR) 22, 27 (1948), English translation, NACA Tech. Memo No. 1282 (1951).

14. Hirschfelder, J.O., Curtiss, C.F., Henkel, M.J., Spaulding, W.F., and Hummel, H., Third Symposium on Combustion and Flame and Explosion Phenomena, The Williams and Wilkins Co., Baltimore, MD, 121-139 (1949).

15. Hirschfelder, J.O., Curtiss, C.F., and Campbell, D.E., Fourth Symposium (International) on Combustion, The Williams and Wilkins Co., Baltimore, MD, 190-211 (1953).

16. Gidding, J.C., and Hirschfelder, J.O., Sixth Symposium (International) on Combustion, Reinhold Publishing Co., NY, 199-213 (1957).

17. Spalding, D.B., Phil. Trans. Roy. Soc. Lond. 249A, 1-25 (1956).

18. Adams, G.K., and Cook, G.B., Combust. Flame 4, 9-18 (1960).

19. Dixon-Lewis, G., Proc. Roy. Soc. Lond. A298, 495-513 (1967).

20. Dixon-Lewis, G., Proc. Roy. Soc. Lond. A307, 111-135 (1968).

21. Dixon-Lewis, G., and Shepherd, I.G., Fifteenth Symposium (International) on Combustion, The Combustion Institute, Pittsburgh, 1483-1491 (1975).

22. Spalding, D.B., Stephenson, P.L., and Taylor, R.G., Combust. Flame 17, 55-64 (1971).

23. Patankar, S.V., and Spalding, D.B., Heat and Mass Transfer in Boundary Layers, 2nd Ed. Intertext Books, London (1970).

24. Spalding, D.B., and Stephenson, P.L., Proc. Roy. Soc. Lond. A324, 315-337 (1971).

25. Tsatsaronis, G., Combust. Flame 33, 217-239 (1978).

26. Smoot, L.D., Hecker, W.C., and Williams, G.A., Combust. Flame 26, 323-342 (1976).

27. Bledjian, L., Combust. Flame 20, 5-17 (1973).

28. Margolis, S.B., J. Comp. Phys. 27, 410-427 (1978).

29. Westbrook, C.K., and Dryer, F.L., Combust. Sci. and Tech. 20, 125-140 (1979).

30. Lund, C.M., A General Computer Program for Calculating Time-Dependent Phenomena Involving One-Dimensional Hydrodynamics, Transport and Detailed Chemical Kinetics, University of California Lawrence Livermore Laboratory Report, UCRL-52504 (1978).

31. Dixon-Lewis, G., Goldsworthy, F.A., and Greenberg, J.B., Proc. Roy. Soc. Lond. A346, 261-278 (1975).

32. Dixon-Lewis, G., Phil. Trans. Roy. Soc. Lond. 292, 5-99 (1979).

33. Dixon-Lewis, G., Combust. Flame. 36, 1-14 (1979).

34. Warnatz, J., Ber. Bunsenges. Phys. Chem. 82, 193-200 (1978).

35. Warnatz, J., Ber. Bunsenges. Phys. Chem. 82, 643-649 (1978).

36. Warnatz, J., Ber. Bunsenges. Phys. Chem. 82, 834-841 (1978).

37. Warnatz, J., Ber. Bunsenges. Phys. Chem. 83, 950-957 (1979).

38. Warnatz, J., Combust. Sci. and Tech. 26, 203-213 (1981).

39. Coffee, T.P., and Heimerl, J.M., A Method for Computing the Flame Speed for a Laminar, Pre-mixed, One-Dimensional Flame, BRL Tech. Rept. ARBRL-TR-02212, Ballistics Research Laboratories, Aberdeen, MD, 1980.

40. Coffee, T.P., and Heimerl, J.M., Combust. Flame 43, 273-289 (1981)

41. Dixon-Lewis, G., Proc. Roy. Soc. Lond. A307, 111-135 (1968).

42. Wilde, K.A., Combust. Flame 18, 43-52 (1972).

43. Smooke, M.D., Solustion of Burner-Stabilized Pre-mixed Laminar Flames by Boundary Value Methods, SAND 81-8040, Sandia National Laboratories, Livermore, CA, 1982.

44. Chapman, S., and Cowling, T.G., The Mathematical Theory of Non-uniform Gases, Cambridge University Press, 1970.

45. Picone, J.M., and Oran, E.S., Approximate Equations for Transport Coefficients of Multicomponent Mixtures of Neutral Gases, NRL Memorandum Report 4384, Naval Research Laboratory, Washington, DC, 1980.

46. Hirschfelder, J.O., Curtiss, C.F., and Bird, R.B., Molecular Theory of Gases and Liquids, John Wiley and Sons, Inc., NY, 1964.

47. Mason, E.A., and Saxena, S.C., Phys. Fluids 1, 361-369 (1958).

48. Hirschfelder, J.O., Sixth Symposium (International) on Combustion, Reinhold Publishing Co., NY, 351-363 (1957).

49. Marrero, T.R., and Mason, E.A., J. Phys. Chem. Ref. Data 1, 3-118 (1972).

50. Burks, T.L., and Oran, E.S., A Computational Study of the Chemical Kinetics of Hydrogen Combuston, NRL Memorandum Report 4446, Naval Research Laboratory, Washington, DC, 1981.

51. Stull, D.R., and Prophet, H., JANAF Thermochemical Tables, National Standard Reference Data Series, National Bureau of Standards, No. 37, 2nd Ed., Gaithersburg, MD, 1971.

52. Oran, E.S., Young, T.R., Boris, J.P., and Cohen, A., Weak and Strong Ignition-I. Numerical Simulations of Shock Tube Experiments, NRL Memorandum Report 4664, Naval Research Laboratory, Washington, DC, 1981. (Also to appear in Combust. Flame).

53. Klein, M., Hanley, H.J.M., Smith, F.J., and Holland, P., Tables of Collision Integrals and Second Virial Coefficients for the (m,6,8) Intermolecular Potential Function, National Standard Reference Data Series, National Bureau of Standards, No. 47, Gaithersburg, MD, 1974.

54. Svehla, R.A., Estimated Viscosities and Thermal Conductivities of Gases at High Temperatures, Technical Report No. R-132, NASA, Washington, DC, 1962.

55. Lewis, B., and von Elbe, G., Combustion, Flames and Explosions of Gases, Academic Press, NY, 1961, pp. 323-367.

56. Baulch, D.L., Drysdale, D.C., Horne, D.C., and Lloyd, A.C., Evaluated Kinetic Data for High Temperature Reactions, Vol. 1, Butterworths, London, 1972.

57. Hampson, R.F., and Garvin, D., Chemical Kinetic and Photochemical Data for Modelling of Atmospheric Chemistry, NBS Technical Note 866, National Bureau of Standards, Washington, DC (1975).

58. Cohen, N., and Westberg, K.R., Data Sheets, The Aerospace Corporation, P.O. Box 92957, Los Angeles, CA (1979).

59. Olson, D.B., and Gardiner, W.C., Jr., J. Phys. Chem. 81, 2514 (1977).

60. Lloyd, A.C., Int. J. Chem. Kinetics 6, 169 (1974).

61. Bahn, G.S., Reaction Rate Compilation for H-O-N System, Gordon and Breach, NY, 1968.


DA
FIL
6-